5 Zou CP, Clifford JL, Xu XC *et al.* Modulation by retinoic acid (RA) of squamous cell differentiation, cellular RA-binding proteins, and nuclear RA receptors in human head and neck squamous carcinoma cell lines. *Cancer Res* 1994; **54**: 5479–87.

6 Campbell MJ, Park S, Uskokovic MR, Dawson MI, Koeffler HP. Expression of retinoic acid receptor-β sensitizes prostate cancer cells to growth inhibition mediated by combination of retinoids and a 19-nor hexafluoride vitamine D3 analogue. *Endocrinology* 1998; **139**: 1972–80.

7 Moon RC, Mehta RG, Rao KVN. Retinoids and cancer in experimental animals. In: Sporn MB, Roberts AB, Goodmann DS, eds. *The Retinoids, Biology, Chemistry, and Medicine*, 2nd edn. New York: Raven Press, 1994; 537–96.

8 Han J. Highlights of the cancer chemoprevention studies in China. *Prev Med* 1993; **22**: 712–22.

9 Petkovich M, Brand NJ, Krust A, Chambon P. A human retinoic acid receptor which belongs to the family of nuclear receptors. *Nature* 1987; **330**: 444–50.

10 de The H, Marchio A, Tiollais P, Dejean A. A novel steroid thyroid hormone receptor-related gene inappropriately expressed in human hepatocellular carcinoma. *Nature* 1987; **330**: 667–70.

11 Brand N, Petkovich M, Krust A *et al.* Identification of a second human retinoic acid receptor. *Nature* 1988; **332**: 850–53.

12 Mangelsdorf DJ, Ong ES, Dyck JA, Evancs RM. Nuclear receptor that identifies a novel retinoic acid response pathway. *Nature* 1990; **345**: 224–9.

13 Mangelsdorf DJ, Borgmeyer U, Heyman RA *et al.* Characterization of three RXR genes that mediate the action of 9-cis-retinoic acid. *Genes Dev* 1992; **6**: 329–44.

14 Leid M, Kastner P, Chambon P. Multiplicity generates diversity in the retinoic acid signalling pathways. *Trends Biochem Sci* 1992; **17**: 427–33.

15 Chambon P. A decade of molecular biology of retinoic acid receptors. *FASEB J* 1996; **10**: 940–54.

16 Qiu H, Zhang W, El-Naggar AK *et al.* Loss of retinoic acid receptor-beta expression is an early event during esophageal carcinogenesis. *Am J Pathol* 1999; **155**: 1519–23.

17 Zhang W, Rashid A, Wu H, Xu XC. Differential expression of retinoic acid receptors and p53 protein in normal, premalignant, and malignant esophageal tissues. *J Cancer Res Clin Oncol* 2001; **127**: 237–42.

18 Xu M, Jin YL, Fu J *et al.* The abnormal expression of retinoic acid receptor-beta, p53 and Ki67 protein in normal, premalignant and malignant esophageal tissues. *World J Gastroenterol* 2002; **8**: 200–2.

19 Kumar A, Kaur J, Chattopadhyay TK, Mathur M, Ralhan R. Differential expression of retinoic acid receptors in normal and malignant esophageal tissues. *J Exp Ther Oncol* 2004; **4**: 1–8.

20 Li M, Song S, Lippman SM *et al.* Induction of retinoic acid receptor-beta suppresses cyclooxygenase-2 expression in esophageal cancer cells. *Oncogene* 2002; **21**: 411–8.

21 Kato H, Tachimori Y, Watanabe H, Igaki H, Nakanishi Y, Ochiai A. Recurrent esophageal carcinoma after esophagectomy with three-field lymph node dissection. *J Surg Oncol* 1996; **61**: 267–72.

22 Lerut T, Nafteux P, Moons J *et al.* Three-field lymphadenectomy for carcinoma of the esophagus and gastroesophageal junction in 174 R0 resections: Impact on staging, disease-free survival, and outcome: A plea for adaptation of TNM classification in upper-half esophageal carcinoma. *Ann Surg* 2004; **240**: 962–74.

23 Sugawara A, Yen PM, Qi Y, Lechan RM, Chin WW. Isoform-specific retinoid-X receptor (RXR) antibodies detect differential expression of RXR proteins in the pituitary gland. *Endocrinology* 1995; **136**: 1766–74.

24 Miki Y, Nakata T, Suzuki T *et al.* Systemic distribution of steroid sulfatase and estrogen sulfotransferase in human adult and fetal tissues. *J Clin Endocrinol Metab* 2002; **87**: 5760–68.

25 Suzuki T, Moriya T, Sugawara A, Ariga N, Takabayashi H, Sasano H. Retinoid receptors in human breast carcinoma: Possible modulators of in situ estrogen metabolism. *Breast Cancer Res Treat* 2001; **65**: 31–40.

26 Ariga N, Moriya T, Suzuki T, Kimura M, Ohuchi N, Sasano H. Retinoic acid receptor and retinoid X receptor in ductal carcinoma in situ and intraductal proliferative lesions of the human breast. *Jpn J Cancer Res* 2000; **91**: 1169–76.

27 Ikeguchi M, Oka S, Gomyo Y, Tsujitani S, Maeta M, Kaibara N. Combined analysis of p53 and retinoblastoma protein expressions in esophageal cancer. *Ann Thorac Surg* 2000; **70**: 913–7.

28 Crowe DL, Hu L, Gudas LJ, Rheinwald JG. Variable expression of retinoic acid receptor (RAR beta) mRNA in human oral and epidermal keratinocytes; relation to keratin 19 expression and keratinization potential. *Differentiation* 1991; **48**: 199–208.

29 Schon M, Rheinwald JG. A limited role for retinoic acid and retinoic acid receptors RAR alpha and RAR beta in regulating keratin 19 expression and keratinization in oral and epidermal keratinocytes. *J Invest Dermatol* 1996; **107**: 428–38.

30 Chakravarti N, Mathur M, Bahadur S, Shukla NK, Rochette-Egly C, Ralhan R. Expression of RARα and RARβ in human oral potentially malignant and neoplastic lesions. *Int J Cancer* 2001; **91**: 27–31.

31 Xu XC, Wong WY, Goldberg L *et al.* Progressive decreases in nuclear retinoid receptors during skin squamous carcinogenesis. *Cancer Res* 2001; **61**: 4306–10.

32 Brabender J, Danenberg KD, Metzger R *et al.* The role of retinoid X receptor messenger RNA expression in curatively resected non-small cell lung cancer. *Clin Cancer Res* 2002; **8**: 438–43.

33 Alfaro JM, Fraile B, Lobo MV, Royuela M, Paniagua R, Arenas MI. Immunohistochemical detection of the retinoid X receptors alpha, beta, and gamma in human prostate. *J Androl* 2003; **24**: 113–9.

34 Tamoto E, Tada M, Murakawa K *et al.* Gene-expression profile changes correlated with tumor progression and lymph node metastasis in esophageal cancer. *Clin Cancer Res* 2004; **10**: 3629–38.

35 Minucci S, Leid M, Toyama R *et al.* Retinoid X receptor (RXR) within the RXR-retinoic acid receptor heterodimer binds its ligand and enhances retinoid-dependent gene expression. *Mol Cell Biol* 1997; **17**: 644–55.

36 Gianní M, Tarrade A, Nigro EA, Garattini E, Rochette-Egly C. The AF-1 and AF-2 domains of RAR gamma 2 and RXR alpha cooperate for triggering the transactivation and the degradation of RAR gamma 2/RXR alpha heterodimers. *J Biol Chem* 2003; **278**: 34458–66.

37 Pogenberg V, Guichou JF, Bourguet W. Purification and crystallization of the heterodimeric complex of RARbeta and RXRalpha ligand-binding domains in the active conformation. *Acta Crystallogr D Biol Crystallogr* 2004; **60**: 1170–72.

38 Rana B, Veal GJ, Pearson AD, Redfern CP. Retinoid X receptors and retinoid response in neuroblastoma cells. *J Cell Biochem* 2002; **86**: 67–78.

HORM CANC (2011) 2:73–81
DOI 10.1007/s12672-010-0062-2

Increased 5α-Reductase Type 2 Expression in Human Breast Carcinoma following Aromatase Inhibitor Therapy: The Correlation with Decreased Tumor Cell Proliferation

Niramol Chanplakorn · Pongsthorn Chanplakorn · Takashi Suzuki · Katsuhiko Ono · Lin Wang · Monica S. M. Chan · Loo Wing · Christopher C. P. Yiu · Louis Wing-Cheong Chow · Hironobu Sasano

Published online: 21 December 2010

Abstract Tumor cell proliferation and progression of breast cancer are influenced by female sex steroids. However, not all breast cancer patients respond to aromatase inhibitors (AI), and many patients become unresponsive or relapse. Recent studies demonstrate that not only estrogens but also androgens may serve as regulators of estrogen-responsive as well as estrogen-unresponsive human breast cancers. However, the mechanism underlying these androgenic actions has remained relatively unknown. Therefore, in this study, we evaluated the effects of AI upon the expression of enzymes involved in intratumoral androgen production including 17β-hydroxysteroid dehydrogenase type 5 (17βHSD5), 5α-reductase types 1 and 2 (5αRed1 and 5αRed2) as well as androgen receptor (AR) levels and correlated the findings with therapeutic responses including Ki67 labeling index (Ki67). Eighty-two postmenopausal invasive ductal carcinoma patients were enrolled in CAAN study from November 2001 to April 2004. Pre- and post-treatment specimens of 29 cases were available for this study. The status of 17βHSD5, 5αRed1, 5αRed2, and Ki67 in pre- and post-treatment specimens were evaluated. The significant increments of 5αRed2 as well as AR were detected in biological response group whose Ki67 LI decreased by more than 40% of the pre-treatment level. This is the first study demonstrating an increment of 5αRed2 and AR in the group of the patients associated with Ki67 decrement following AI treatment. These results suggest that increased 5αRed2 and AR following AI treatment may partly contribute to reduce the tumor cell proliferation through increasing intratumoral androgen concentrations and its receptor.

Keywords Breast cancer · Androgen · Androgen receptor · 5α-reductase · Aromatase inhibitor · Ki67

N. Chanplakorn · T. Suzuki · K. Ono · L. Wang · M. S. M. Chan · L. Wing · C. C. P. Yiu · H. Sasano (✉)
Department of Pathology, Tohoku University School of Medicine,
2-1 Seiryou-machi, Aoba-Ku,
Sendai, Miyagi 980-8575, Japan
e-mail: hsasano@patholo2.med.tohoku.ac.jp

N. Chanplakorn
Department of Pathology, Faculty of Medicine,
Ramathibodi Hospital, Mahidol University,
Bangkok, Thailand

P. Chanplakorn
Department of Orthopaedic, Faculty of Medicine,
Ramathibodi Hospital, Mahidol University,
Bangkok, Thailand

M. S. M. Chan · L. Wing · C. C. P. Yiu · L. Wing-Cheong Chow
Comprehensive Centre for Breast Diseases,
UNIMED Medical Institute,
Hong Kong, China

Introduction

Breast cancer is the most common malignancy among women worldwide and the leading cause of cancer-related death in many countries [1, 2]. Hormones, especially sex steroid hormones, play a pivotal role in endocrine-mediated tumorigenesis and have been demonstrated to influence carcinoma cell growth and progression [3, 4]. Among these sex steroids, estrogens, especially estradiol or E2, a biologically potent estrogen, has been demonstrated to play pivotal roles in cell proliferation, development, and invasion of these hormone-dependent breast carcinoma cells [4, 5]. Aromatase inhibitors (AI) have been demonstrated to be more effective and to have fewer side effects in estrogen receptor (ER)-positive breast cancer patients than the

conventional anti-estrogen tamoxifen [6–8]. However, some patients did not respond to this therapy or developed clinical resistance during the course of this therapy [9]. Therefore, it becomes very important to evaluate the mechanisms of these clinical resistances to AI therapy in estrogen receptor positive breast cancer patients. Results of several previous studies demonstrated that androgens exert opposing effects upon the growth and development as well as upon an inhibition of the proliferation of breast carcinoma cells [10, 11], although some controversies existed [12]. In addition, estrogens and androgens have been both reported to be locally produced in breast carcinoma tissue in an intracrine manner [13, 14]. Androgen receptor (AR) is commonly expressed in human breast carcinoma tissues [15]. These data of in situ production of androgen and the presence of AR in breast carcinoma suggest potentially important roles of androgens in breast carcinomas. In particular, androgen producing enzymes, such as 17β-hydroxysteroid dehydrogenase type 5 (17βHSD5; conversion from circulating androstenedione to testosterone) and 5α-reductase types 1 and 2 (5αRed1 and 5αRed2, respectively; reduction of testosterone to 5α-dihydrotestosterone (DHT)) have been reported to be abundantly expressed in breast carcinoma tissues [16]. Especially, in situ production of DHT has been reported in breast cancer tissues [17]. This locally produced DHT then binds with the highest affinity to AR and promotes AR transcriptional activity [16].

We have previously demonstrated an association between the status of intratumoral androgenic enzymes, 5αRed1, and DHT concentration in the breast carcinoma tissue and an inverse correlation between intratumoral DHT concentration and aromatase expression in cell culture experiments [17]. Results of our previous study above indicated that aromatase, whose substrates include testosterone, may act as a negative regulator for in situ production of DHT in breast carcinoma tissue. Therefore, the alterations of these in situ androgen metabolisms following AI treatment can provide very important information toward a better understanding of the changes of local endocrine environment associated with estrogen depletion. Especially, the comparison of the specimens between pre- and post-AI treatment in neoadjuvant therapy may provide important information as to the changes of intratumoral intracrine environment caused by AI. We have recently reported significant increment of the enzymes; estrogen sulfatase and 17β-hydroxysteroid dehydrogenase type 1, the enzymes also involved in intratumoral estrogen production, following AI therapy, which may represent the compensatory response of breast carcinoma tissues to estrogen deprivation state [18]. In addition, Takagi et al. has also recently demonstrated the increment of intratumoral DHT concentration and17β-hydroxysteroid dehydrogenase type 2 (17βHSD2) expressions in breast carcinoma tissues following exemestane treatment and further reported that 17βHSD2 expression was induced by both DHT and exemestane in a dose dependent fashion in their in vitro studies [19]. However, to the best of our knowledge, the alterations of major androgen producing enzymes such as 17βHSD5, 5αRed1, and 5αRed2 before and after AI treatment of breast cancer patients have not been reported at all (Figs. 1 and 2).

Therefore, in this study, we evaluated the alterations of these enzymes including 17βHSD5, 5αRed1 and 5αRed2, and AR expression in breast carcinoma tissue before and after the neoadjuvant AI treatment using the immunohistochemistry (IHC). We then correlated the obtained findings with the alteration of Ki67 of individual patients and the changes of ER, progesterone receptor (PgR), and human epidermal growth factor receptor type 2 (Her2) in breast carcinoma tissues before and after the therapy in order to further understand these changes of intratumoral androgen producing pathways. In particular, we evaluated the clinical and biological significance of intratumoral androgenic enzymes, especially 5αRed2, in association with the decreased Ki67 from estrogen depletion caused by AI therapy.

Materials and Methods

Breast Carcinoma Cases

The specimens available for examinations in this study were pre- and post-treatment samples obtained from Celecoxib Anti-aromatase Neoadjuvant trial (CAAN trial). This was a neoadjuvant clinical trial conducted, from November 2001 to April 2004, at The University of Hong Kong and Queen Mary Hospital, Hong Kong [20]. The study design had been reported previously [20] but, in brief, all 82 patients enrolled in this neoadjuvant study were postmenopausal women with histological proof of invasive ductal breast carcinoma and positive ER/PgR status determined by the IHC analysis [20]. Informed consents had been obtained from all the patients prior to their enrollment into this trial, which had been approved by the local ethics committee. In CAAN trial study, it was conducted to investigate the efficacy and safety of neoadjuvant therapy combining AI with COX-2 inhibitor. According to the protocol of CAAN trial, the patients were randomly assigned to receive exemestane 25 mg daily and celecoxib 400 mg twice daily (group A, n=30), exemestane 25 mg daily (group B, n=24) and letrozole 2.5 mg daily (group C, n=28), respectively. Each patient was treated for 3 months and surgery was performed within 7 days after the treatment. As reported previously, there were no significant

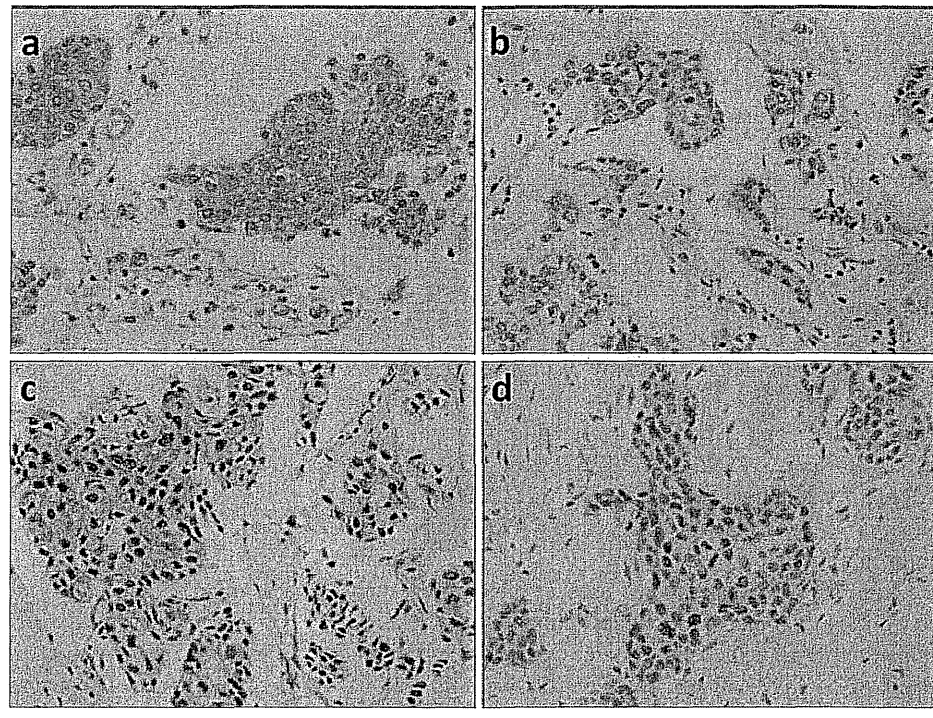

Fig. 1 Representative illustrations of immunohistochemistry: 17βHSD5 (**a**), 5αRed1 (**b**), 5αRed2 (**c**), and AR (**d**) in one case of invasive ductal carcinoma. Immunoreactivity of 17βHSD5, 5αRed1, and 5αRed2 were detected in the cytoplasm of invasive ductal carcinoma cells while those of AR in the nucleus. Original magnification, ×200

differences in term of clinical and pathological responses among these three different treatment groups [20]. Therefore, the responses toward AI therapy were by no means influenced by the concurrent use of celecoxib.

The pre- and post-treatment specimens of 29 patients were available for this pathological response and IHC evaluation study. According to the protocol of CAAN trial, these 29 patients were randomly assigned to receive the treatment as follows (group A, n=10; group B, n=8; and group C, n=11). Their mean age was 74.6 years (range, 51–93 years).

Pathological Response

Tissue sections of the same tumors from pre-treatment core needle biopsies and final surgical specimens were obtained and assessed for the changes in cellularity and degree of fibrosis in hematoxylin–eosin-stained slides. Pathological response was categorized, using the modified criteria described by Miller et al. [21] and assessed as follows: complete when there was no evidence of carcinoma cell at the original tumor site; partial response when histological decrement in cellularity and/or increment in fibrosis was

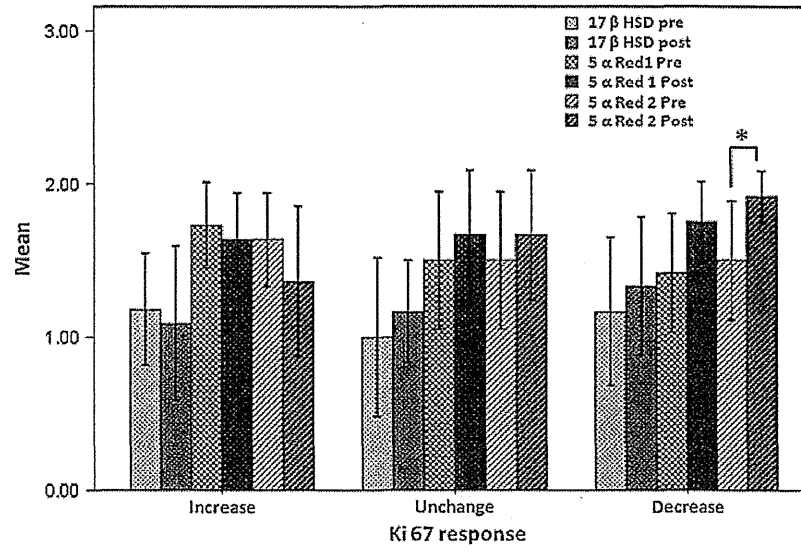

Fig. 2 Demonstration of the mean value of the intratumoral androgenic enzymes before and after the AI treatment grouped by the Ki67 LI response. *Error bar* represents ±2 standard error of measurement (SEM). *P<0.05, significant difference between pre- and post-treatment values

detected; or no change/nonresponse, by two of the authors above (NC and MC).

Immunohistochemistry

All immunohistological investigations were performed on the pre-treatment core needle biopsies and final surgical specimens. One 4-μm section of each submitted paraffin blocks of pre- and post-treatment specimens were stained with hematoxylin–eosin to verify an adequate number of invasive breast carcinoma cells and the quality of fixation in order to determine the suitability of further IHC analysis. In brief, serial tissue sections (4-μm) were prepared from selected blocks and IHC was performed to immunolocalize ER, PgR, Her2, Ki67, AR, 17βHSD5, 5αRed1, and 5αRed2, as described previously [17, 22]. A Histofine Kit (Nichirei, Tokyo, Japan), which employs the streptavidin-biotin amplification method, was used for IHC staining. The lists of primary antibodies used in our present study, the working dilutions of individual antibodies, the details of antigen retrieval methods, the sources of antibodies and the details of positive and negative controls were all summarized in Table 1. The antigen–antibody complex was visualized with 3, 3′-diaminobenzidine (DAB) solution (1 mM DAB, 50 mM Tris–HCl buffer (pH 7.6), and 0.006% H_2O_2), and counterstained with hematoxylin.

The immunostained slides were independently evaluated by two of the authors (NC and TS), blinded to clinical outcome of individual patients. 17βHSD5, 5αRed1 and 5αRed2 immunoreactivity were evaluated using a semi-quantitative method as follows: score 2, >50% positive cells; score 1, 1–50% positive cells; and score 0, no immunoreactivity, as previously described by Suzuki et al. [23]. Evaluation of Ki67 was performed by counting of 1,000 carcinoma cells or more from each cases and the percentage of immunoreactivity was subsequently determined as a labeling index (LI) [24].

In addition, the Ki67 LI was then subclassified, using the criteria reported by Miller et al. [21], into three different groups according to the percentage of Ki67 alterations after treatment as follows: group1; increased group, the Ki67 LI in this group was associated with an increment after therapy, group2; no change group, the Ki67 LI demonstrated unchanged or reduction for less than 40% of the pre-treatment level, group3; decreased group, the Ki67 LI demonstrated the reduction for more than 40% of the pre-treatment level. ER, PgR, and AR immunoreactivity were scored by assigning proportion and intensity scores, according to Allred's procedure [25]. In brief, a proportion score represented the estimated proportion of immunopositive tumor cells as follows: 0 (none), 1 (<1/100), 2 (1/100 to 1/10), 3 (1/10–1/3), 4 (1/3 to 2/3), and 5 (>2/3). An intensity score represented the average immunointensity of the positive cells as follows: 0 (none), 1 (weak), 2 (intermediate), and 3 (strong). Any nuclear discernible immunoreactivity in breast carcinoma cells were counted toward both proportion and intensity scores. The proportion and intensity scores were then added to obtain a total score that could range from 0 to 8.The membrane staining pattern was estimated in Her2 IHC and scored on a scale of 0 to 3 [26].

Statistical Analysis

The Kruskal–Wallis test was used to compare the pre-treatment IHC scores of all biological markers according to three groups of AI treatment in individual patients. The Wilcoxon matched-pairs signed ranks test was employed in order to determine the mean differences between pre- and post-treatment IHC scores of individual biological markers in relation to the pathological responses status and the alterations of Ki67 LI. The correlations among intratumoral androgenic enzymes (17βHSD5, 5αRed1, and 5αRed2) before and after AI treatment were analyzed using Spearman's rank nonparametric correlation test. Logistic regression analysis was conducted to determine whether the

Table 1 The list of antibodies employed for immunostaining in this study

Biological markers	Dilution	Pre-treatment method for antigen retrieval	Providers	Positive and negative controls
AR	1:50	Autoclave in citrate buffer	Dako, Denmark	Prostate gland
17βHSD5	1:200	Not required	Sigma	Testis
5αRed1	1:2,000	Not required	–[a]	Liver
5αRed2	1:1,000	Not required	–[a]	Liver
Ki67	1:100	Autoclave in citrate buffer	Dako, Denmark	Breast cancer
ER	Undiluted	Pre-treatment by heat in automated machine	Roche diagnostic, Germany	Breast cancer
PgR	Undiluted	Pre-treatment by heat in automated machine	Roche diagnostic, Germany	Breast cancer
Her2	Undiluted	Pre-treatment by heat in automated machine	Roche diagnostic, Germany	Breast cancer

AR androgen receptor, *17βHSD5* 17β-hydroxysteroid dehydrogenase type 5, *5αRed1* 5αreductase type 1, *5αRed2* 5αreductase type 2, *Ki67* Ki67 protein, *ER* estrogen receptor, *PgR* progesterone receptor, *Her2* human epidermal growth factor receptor type 2

[a] Kindly provided by Dr. D.W. Russell (University of Texas Southwestern Medical Center, Dallas, Texas)

Table 2 The alterations of biological markers before and after the aromatase inhibitors treatment

Biological markers	Pre-treatment value (mean (SEM))	Post-treatment value (mean (SEM))	Mean difference (95% CI)	*p* value
17βHSD5	1.138 (0.128)	1.207 (0.135)	−0.06879 (−0.3165, 0.1786)	0.6221
5αRed1	1.552 (0.106)	1.689 (0.087)	−0.1379 (−0.3811, 0.1052)	0.3394
5αRed2	1.552 (0.106)	1.655 (0.114)	−0.1034 (−0.3971, 0.1902)	0.5771
AR	6.103 (0.295)	6.862 (0.242)	−0.7586 (−1.3210, −0.1959)	0.0127*
ER	7.034 (0.202)	7.586 (0.105)	−0.5517 (−0.9780, −0.1255)	0.015*
PgR	6.965 (0.195)	5.862 (0.321)	1.103 (0.3967, 1.810)	0.0017*
Her 2	1.758 (0.146)	1.586 (0.168)	0.1724 (−0.1163, 0.4661)	0.2958
Ki67	16.352 (1.902)	12.162 (1.754)	4.19 (0.1332, 8.246)	0.0439*

Data showed by mean (standard error of measurement (SEM) of the IHC score of the pre- and post-treatment values; mean difference (pre- and post-treatment values) with 95% confidence interval (lower and upper values) *p* value calculated by Wilcoxon's matched-pairs signed-rank test

17βHSD5 17β-hydroxysteroid dehydrogenase type 5, *5αRed1* 5αreductase type 1, *5αRed2* 5αreductase type 2, *AR* androgen receptor, *ER* estrogen receptor, *PgR* progesterone receptor, *Her2* human epidermal growth factor receptor type 2, *Ki67* Ki67 protein

*p value<0.05

changes in androgenic enzymes, especially 5αRed2, predicted for decreased Ki67 LI or response group. The statistically significance was considered the p value<0.05.

Results

Biopsies from 29 patients who had been treated with exemestane and celecoxib (group A, n=10), exemestane (group B, n=8), or letrozole (group C, n=11), were available for evaluation of pathological response assessment and IHC studies. Pathological responders and nonresponders were 7 (24.1%) and 22 cases (75.9%), respectively.

Immunohistochemistry

The median of pre-treatment individual biological markers were compared but demonstrated no statistical significance (Nonparametric ANOVAs; Data not shown). We then analyzed the changes of IHC scores of all biological markers after the treatment. The statistically significant reduction in PgR expression and Ki67 LI were detected (p=0.0017 and p=0.0439, respectively), as previously reported in letrozole [21], anastrozole [27], and exemestane [22] neoadjuvant treatment but the expression levels of both ER and AR were increased (p=0.015 and p=0.0127, respectively). In addition, the expressions of intratumoral androgenic enzymes were increased but theses increments did not reach statistical significance (Table 2).

An Association of Alterations of Intratumoral Androgenic Enzymes and Ki67 LI

Differences of the individual enzymes and other biological markers between pre- and post-treatment were evaluated according to those categories of Ki67 LI described above.

Table 3 The changes in biological markers after the aromatase inhibitors treatment grouped by the changes of Ki67 labeling index

Biological markers	Ki67 increased (n=11)		Ki67 unchanged (n=6)		Ki67 decreased (n=12)	
	Mean difference (95% CI)	*p* value	Mean difference (95% CI)	*p* value	Mean difference (95% CI)	*p* value
17βHSD5	0.0909 (−0.3798, 0.5616)	0.655	−0.1667 (−0.9568, 0.6234)	0.564	−0.1667 (−0.5335, 0.2002)	0.317
5αRed1	0.0909 (−0.2714, 0.4532)	0.564	−0.1667 (−0.9568, 0.6234)	0.564	−0.3333 (−0.7472, 0.08051)	0.102
5αRed2	0.2727 (−0.3349, 0.8804)	0.276	−0.1667 (−0.9568, 0.6234)	0.564	−0.4167 (−0.7438, −0.08949)	0.025*
AR	−0.8182 (−1.935, 0.2986)	0.164	−0.3333 (−1.604, 0.9378)	0.625	−0.9167 (−1.8730, 0.0396)	0.039*
ER	−0.6364 (−1.257, −0.01537)	0.053	−1.000 (−2.878, 0.8776)	0.197	−0.250 (−0.8003, 0.3003)	0.317
PgR	0.000 (−0.6008, 0.6008)	1.000	1.000 (−0.3277, 2.328)	0.098	2.167 (0.7633, 3.570)	0.005*
Her 2	0.000 (−0.5203, 0.5203)	1.000	0.3333 (−0.2087, 0.8753)	0.157	0.250 (−0.3003, 0.8003)	0.317

Data demonstrated by mean difference (pre- and post-treatment values) with 95% confidence interval (lower and upper values); *p* value calculated by Wilcoxon's matched-pairs signed-rank test

n sample in each group, *17βHSD5* 17β-hydroxysteroid dehydrogenase type 5, *5αRed1* 5αreductase type 1, *5αRed2* 5αreductase type 2, *AR* androgen receptor, *ER* estrogen receptor, *PgR* progesterone receptor, *Her2* human epidermal growth factor receptor type 2. *Ki67* Ki67 protein

*p value<0.05

Immunoreactivity of ER, PgR, Her2, AR, 17βHSD5, 5αRed1, and 5αRed2 in pre-treatment specimens were not significantly different among these three different groups of Ki67 LI changes (nonparametric ANOVAs; data not shown). In group 1 or whose Ki67 LI increased after the therapy and group 2 or whose Ki67 LI unchanged or decreased with less than 40% of the pre-treatment level, no statistically significant difference was detected among any of intratumoral enzymes and biomarkers examined between the specimens before and after the treatment. In group 3 or whose Ki67 LI decreased with more than 40% of the pre-treatment level, the significant increment of 5αRed2 and AR and decrement of PgR expression were demonstrated in this study (p=0.025, p=0.039, and p=0.005, respectively), whereas the expression of other biological markers did not show any statistically significances (Table 3).

Correlation Among Intratumoral Androgenic Enzymes Before and After AI Treatment

We then examined the correlation between IHC scores of intratumoral enzymes in tumors before and after the treatment according to the categories of Ki67 LI. In pre-treatment group of the patients, androgenic enzymes including 17βHSD5, 5αRed1 and 5αRed2, were significantly correlated with each other (Table 4). Those correlations were, however, changed following AI treatment. In group 1 or whose Ki67 LI increased after the therapy, 17βHSD5 was still correlated with 5αRed2 (p=0.009) as well as 5αRed1 with 5αRed2 (p=0.001) but loss of correlation between 17βHSD5 and 5αRed1 was detected (p=0.067). In group 2 or whose Ki67 LI unchanged or decreased with less than 40% of the pre-treatment level, only the correlation between 5αRed1 and 5αRed2 remained significant. The level of statistical significance was not reached in group 3 or those Ki67 LI decreased by more than 40% of the pre-treatment level (Table 4).

The Relative Importance of Androgenic Enzymes on Ki67 LI Decrement by AI Treatment

We further evaluated the effects of alterations of androgenic enzymes to determine whether these alterations, especially those of 5αRed2, were correlated with the status of response or nonresponse to the AI treatment determined by Ki67 LI changes. The status of each androgenic enzymes in post-treatment was further subclassified into three different groups according to the level of their changes after the treatment as follows: group 1; increased group, the status of the enzymes in this group was associated with an increment compared to the pre-treatment level. Group 2; no change group, the status of the enzymes was the same as that in the pre-treatment level. Group3; decreased group, the status of enzymes was

Table 4 The correlation between biological markers involve in androgen production before and after the treatment with aromatase inhibitors grouped by the changes in Ki 67 labeling index

Biological markers	Post-treatment							
	Before treatment (n=29)		Ki67 increased (n=11)		Ki67 unchanged (n=6)		Ki67 decreased (n=12)	
	5αRed1	5αRed2	5αRed1	5αRed2	5αRed1	5αRed2	5αRed1	5αRed2
17βHSD5	0.59 (0.001)*	0.695 (0.00)*	0.57 (0.067)	0.743 (0.009)*	0.316 (0.541)	0.316 (0.541)	0.243 (0.446)	0.477 (0.117)
5αRed1		0.87 (0.00)*		0.859 (0.001)*		1.000 (0.000)*		0.522 (0.082)

Data demonstrated by the correlation coefficient with (p value) calculated by Spearman's rank correlation

n samples in each group, *17βHSD5* 17β-hydroxysteroid dehydrogenase type 5, *5αRed1* 5αreductase type 1, *5αRed2* 5αreductase type 2, *Ki67* Ki67 protein

*p value<0.05

decreased following the therapy. We could not find any significance among these groups in the logistic regression analysis (Table 5).

Discussion

Numerous studies have been reported on the possible roles of androgens in human breast cancer but it is also true that controversies exist as to clinical or biological significance of androgens, especially in estrogen dependent breast cancer [10–14, 17, 19, 22]. Previously, Sonne–Hansen and Lykkesfeldt reported the presence of a significant aromatase activity in the MCF-7 cells and this activity was also reported to be sufficient for the breast carcinoma cells to aromatize testosterone to estrogen, which resulted in significant cell growth stimulation [14]. In addition, both the steroidal and nonsteroidal aromatase inhibitors were reported to be able to completely abolish the growth-stimulatory effects of testosterone [14]. However, Macedo et al. reported that androgens, such as androstenedione and 5α-DHT, inhibited MCF-7 cell proliferation in a low-estrogen milieu and letrozole treatment did inhibit breast carcinoma cell proliferation by inhibiting the conversion of androgens to estrogen, and subsequently making androgens available to exert their anti-proliferative effects possibly through up-regulation of AR [10].

We also demonstrated statistically significant AR increment following the AI treatment, which is consistent with the results of previous reported studies above, but it is also true that Yamashita et al. did not detect this change during the exemestane treatment [22]. In addition, Suzuki et al. recently reported that intratumoral DHT of human breast carcinoma tissues was mainly determined by the status of 5αRed1 and aromatase [28]. In our present study, we demonstrated the correlation between the effects of AI treatment and the changes of androgenic enzymes expression. The significant correlation was also detected between the decrement in Ki67 LI or biological response of the AI treatment and the increment of 5αRed2 following AI administration in breast carcinoma patients.

Locally produced estrogens play a major role in proliferation of estrogen dependent breast cancer and androgens are considered to predominantly exert anti-proliferative effects via AR [15]. Intratumoral estrogens can be produced from circulating androgens, especially those derived from the zona reticularis of an adrenal cortex, catalyzed by the aromatase enzyme in which the neo-adjuvant AI treatment blocks this enzyme with immense potency and exquisite specificity [6]. We previously demonstrated an increment of the intratumoral enzymes following AI therapy in the compensatory direction toward increasing intratumoral estrogen production [18]. However, the alteration of androgen metabolizing enzymes as a result of the neoadjuvant hormonal breast cancer therapy has not been examined at all.

Local androgen concentration has been well known to be significantly increased in breast cancer by AI treatment, as previously reported in various in vitro studies [10–12, 17, 29]. Takagi et al. recently demonstrated an increment of DHT concentration in breast carcinoma tissue following the exemestane therapy as well as the inhibitory effects of DHT on estradiol-mediated T-47D cells proliferation [19]. These findings all suggested that AI not only suppress aromatase enzyme and cause estrogen depletion in consequence, but also provide additional effects through increasing local DHT concentration, which may result in decreased cell proliferation of tumor cells. These findings were consistent with results of our present study that the statistically significant increment of 5αRed2 enzyme was detected only in the group associated with reduction of Ki67 LI with more than 40% of the pre-treatment level or group 3 (p=0.025) (Table 3). Following AI treatment, an accumulation of in situ androgens in breast cancer tissues may occur and the enzyme 5αRed2 can serve as an important regulator of local actions of androgens because this enzyme converts testosterone into the biologically more active and nonaromatizable DHT [4, 11, 17]. However, further studies such as the analysis of much larger number of neoadjuvant treated patients are required for confirmation of this interesting hypothesis.

The potent and direct inhibitory effects of DHT on human breast cancer cell proliferation were first demonstrated by Poulin et al. in 1988 [30]. Two isoforms of

Table 5 Odds ratio of each androgenic enzymes related to the Ki67 labeling index alterations following the aromatase inhibitors treatment

Biological markers	Post-treatment IHC status	Odds ratio (95% CI)	p value
17βHSD5	Increased	0.368 (0.028, 4.746)	0.443
	Unchanged	Reference	
	Decreased	0.696 (0.045, 10.766)	0.795
5αRed1	Increased	1.644 (0.156, 17.359)	0.679
	Unchanged	Reference	
	Decreased	Cannot be calculated	1.000
5αRed2	Increased	3.739 (0.177, 79.081)	0.397
	Unchanged	Reference	
	Decreased	0.000 (0.000, –)	0.999

Data showed the odds ratio of the Ki67 response with (95% confidence interval) and p value calculated by logistic regression analysis; post-treatment IHC status means the change in the IHC scores after the treatment; the unchanged of IHC scores after treatment were used as reference for the comparison

17βHSD5 17β-hydroxysteroid dehydrogenase type 5, *5αRed1* 5α-reductase type 1, *5αRed2* 5αreductase type 2, *Ki67* Ki67 protein

5αRed have been known to exist, encoded by different genes: SRD5A1 (chromosome 5p15) and SRD5A2 (chromosome 2p23) [31, 32]. The two types of 5αRed share 50% amino acid sequence identity and possess similar substrate specific but have different optimal pH and sensitivity to inhibitors [32]. 5αRed2 is the major form of the enzyme expressed in the human prostate [32] but rarely detected in human breast carcinoma [28]. Both Wiebe et al. [33] and Suzuki et al. [17, 28] demonstrated the expression of 5αRed1 in several types of human breast cancer cell lines using semi-quantitative RT-PCR and in human breast carcinoma tissues using IHC and RT-PCR, respectively. In addition, significant increment of 5αRed1 and 5αRed2 genes expression of human breast carcinoma as compared to normal breast tissue has been illustrated in the semi-quantitative RT-PCR study [34]. However, the regulatory mechanisms of 5αRed2 in human breast carcinoma have remained largely unknown and it awaits further investigations for clarification.

In our present study, we did not, however, detect the significant alterations in the enzymes involved in androgen metabolism in non response groups (groups 1 and 2) (Table 3). This finding suggests that androgen metabolism is not influenced by the AI treatment in these groups of patients with breast cancer or nonresponders. The loss of correlation of intratumoral androgenic enzymes in breast carcinoma tissue; 17βHSD5, 5αRed1, and 5αRed2, after AI treatment (Table 4) as well as the alterations of 5αRed1 and 5αRed2 enzymes (Table 2) were detected, but these changes did not reach statistical significance. This may be due to the relatively small size of the patients examined, especially the rather limited number of available specimens in our present study. In addition, the breast carcinoma cases associated with greater reduction of Ki67 LI tended to be associated with an increased 5αRed2, but this correlation did not reach statistical significance (Table 5).

After menopause, most of the biologically active androgens (as well as estrogens) are synthesized in peripheral intracrine tissues, for example in the breast, from precursors of adrenal origin without release of active androgens in the extracellular space and the circulation [4, 11]. In addition, DHT concentrations were demonstrated to be significantly higher in breast cancer tissues than in plasma [35]. In addition, both 17β-hydrosteroid dehydrogenase and 5α-reductases have been considered to act to increase DHT production by competing with aromatase for substrates in hormone-dependent breast carcinoma [19, 28]. As mentioned above, 5αRed1 is the predominant form of 5α-reductases at least in human breast cancer [17, 28, 32], but the results of our present study clearly demonstrate the importance of 5αRed2, which is rarely expressed in breast cancer but was increased in response group or those associated with more Ki67 decrement. We therefore hypothesized that this rather de novo 5αRed2 increment may be related to the effects of AI other than depleting in situ estrogens, i.e., the potential increment of the endogenous androgens which may exert their anti-proliferative effects via the AR, especially in a low-estrogen milieu, as demonstrated in the breast cancer cell lines study [10] and possibly to an induction in apoptosis signaling pathways. Androgens, androstenedione, and DHT, were reported to have a proapoptotic effect by strongly reducing Bcl-2 expression in MCF-7 cells, and this androgenic inhibitory effect was mediated via the AR [10, 36].

In summary, this is the first study which demonstrates an alteration of the androgen producing enzymes following the AI treatment, especially a de novo increment of 5αRed2 as well as of AR may be considered at least one of the mechanisms to account for the decreased breast carcinoma cell proliferation after AI therapy through an increment of local concentrations of androgens and their actions. However, the regulatory mechanisms of 5αRed2 in human breast carcinoma have remained largely unknown.

Acknowledgment We thank Dr. D.W. Russell (University of Texas Southwestern Medical Center, Dallas, Texas) for kindly providing antibodies against 5αRed1 and 5αRed2.

Disclosures/Conflicts of interest Dr. Hironobu Sasano has received the educational research grant from Novartis Oncology Japan and Pfizer Oncology Japan.

References

1. Garcia M, Jemal A, Ward EM, Center MM, Hao Y, Siegel RL, Thun MJ (2007) Global Cancer Facts & Figures 2007. Atlanta, GA: *American Cancer Society.* Available at: http://www.cancer.org/docroot/STT/STT_0.asp. Accessed 19 Nov 2009
2. American Cancer Society (2009) Breast Cancer Facts & Figures 2009–2010. Atlanta, GA: *American Cancer Society.* Available at: http://www.cancer.org/docroot/STT/STT_0.asp. Accessed Nov 2009
3. Pasqualini JR, Chetrite GS (2005) Recent insight on the control of enzymes involved in estrogen formation and transformation in human breast cancer. J Steroid Biochem Mol Biol 93:221–236
4. Sasano H, Nagasaki S, Miki Y, Suzuki T (2009) New developments in intracrinology of human breast cancer estrogen sulfatase and sulfotransferase. Ann NY Acad Sci 1155:76–79
5. Miller WR, Forrest AP (1974) Oestradiol synthesis by a human breast carcinoma. Lancet 2:866–868
6. Miller WR, Anderson TJ, White S, Larionov A, Murray J, Evans D, Krause A, Dixon JM (2005) Aromatase inhibitors: cellular and molecular effects. J Steroid Biochem Mol Biol 95:83–89
7. Geisler J (2008) Aromatase inhibitors: from bench to bedside and back. Breast Cancer 15:17–26
8. Geisler J, LØnning PE (2005) Aromatase inhibition: translation into a successful therapeutic approach. Clin Cancer Res 11: 2809–2821
9. Chen S, Masri S, Hong YY, Wang X, Phung S, Yuan YC, Wu X (2007) New experimental models for aromatase inhibitor resistance. J Steroid Biochem Mol Biol 106:8–15

10. Macedo LF, Guo Z, Tilghman SL, Sabnis GJ, Qiu Y, Brodie A (2006) Role of Androgens on MCF-7 breast cancer cell growth and on the inhibitory effect of letrozole. Cancer Res 66(15):7775–7782
11. Labrie F, Luu-The V, Labrie C, Bélanger A, Simard J, Lin SX, Pelletier G (2003) Endocrine and intracrine sources of androgens in women: inhibition of breast cancer and other roles of androgens and their precursor dehydroepiandrosterone. Endocr Rev 24:152–182
12. Lippman M, Bolan G, Huff K (1976) The effect of androgens and antiandrogens on hormone-responsive human breast cancer in long-term tissue culture. Cancer Res 36:4610–4618
13. Miller WR, McDonald D, Forrest AP, Shivas AA (1973) Metabolism of androgens by human breast tissue. Lancet 1:912–913
14. Sonne-Hansen K, Lykkesfeldt AE (2005) Endogenous aromatization of testosterone results in growth stimulation of the human MCF-7 breast cancer cell line. J Steroid Biochem Mol Biol 93:25–34
15. Moinfar F, Okcu M, Tsybrovskyy O, Regitnig P, Lax SF, Weybora W, Ratschek M, Tavassoli FA, Denk H (2003) Androgen receptors frequently are expressed in breast carcinomas. Cancer 98:703–711
16. Sasano H, Suzuki T, Miki Y, Moriya T (2008) Intracrinology of estrogens and androgens in breast carcinoma. J Steroid Biochem Mol Biol 108:181–185
17. Suzuki T, Miki Y, Moriya T, Akahira J, Ishida T, Hirakawa H, Yamakuchi Y, Hayashi S, Sasano H (2006) 5α-Reductase type 1 and aromatase in breast carcinoma as regulators of in situ androgen production. Int J Cancer 120:285–291
18. Chanplakorn N, Chanplakorn P, Suzuki T, Ono K, Chan SMM, Miki Y, Saji S, Ueno T, Toi M, Sasano H (2010) Increased estrogen sulfatase (STS) and 17β-hydroxysteroid dehydrogenase type 1(17β-HSD1) following neoadjuvant aromatase inhibitor therapy in breast cancer patients. Breast Cancer Res Treat 120 (3):639–648
19. Takagi K, Miki Y, Nagasaki S, Hirakawa H, Onodera Y, Akahira J, Ishida T, Watanabe M, Kimijima I, Hayashi S, Sasano H, Suzuki T (2010) Increased intratumoral androgens in human breast carcinoma following aromatase inhibitor exemestane treatment. Endocr-Relat Cancer 17(2):415–430
20. Chow LWC, Yip AYS, Loo WTY, Lam CK, Toi M (2008) Celecoxib anti-aromatase neoadjuvant (CAAN) trial for locally advanced breast cancer. J Steroid Biochem Mol Biol 111:13–17
21. Miller WR, White S, Dixon JM, Murray J, Renshaw L, Anderson TJ (2006) Proliferation, steroid receptors and clinical/pathological response in breast cancer treated with letrozole. Br J Cancer 94:1051–1056
22. Yamashita H, Takahashi S, Ito Y, Yamashita T, Yoshiaki A, Toyama T, Sugiura H, Yoshimoto N, Kobayashi S, Fujii Y, Iwase H (2009) Predictors of response to exemestane as primary endocrine therapy in estrogen receptor-positive breast cancer. Cancer Sci 100:2028–2033
23. Suzuki T, Moriya T, Ariga N, Kaneko C, Kanazawa M, Sasano H (2000) 17beta-hydroxysteroid dehydrogenase type 1 and type 2 in human breast carcinoma: a correlation to clinicopathological parameters. Br J Cancer 82:518–523
24. Bouzubar N, Walker KJ, Griffiths K, Ellis IO, Elston CW, Robertson JFR, Blamey RW, Nicholson RI (1989) Ki67 immunostaining in primary breast cancer: pathological and clinical associations. Br J Cancer 59:943–947
25. Harvey JM, Clark GM, Osborne CK, Allred DC (1999) Estrogen receptor status by immunohistochemistry is superior to the ligand-binding assay for predicting response to adjuvant endocrine therapy in breast cancer. J Clin Oncol 17:1474–1481
26. Wolff AC, Hammond ME, Schwartz JN et al (2007) American Society of Clinical Oncology/College of American Pathologists guideline recommendations for human epidermal growth factor receptor 2 testing in breast cancer. J Clin Oncol 25:118–145
27. Dowsett M, Ebbs SR, Dixon JM, Skene A, Griffith C, Boeddinghaus I, Salter J, Detre S, Hills M, Ashley S, Francis S, Walsh G, Smith IE (2005) Biomarker changes during neoadjuvant anastrozole, tamoxifen, or the combination: influence of hormonal status and Her-2 in breast cancer-a study from the IMPACT trialists. J Clin Oncol 23:2477–2492
28. Suzuki T, Darnel AD, Akahira J, Ariga N, Ogawa S, Kaneko C, Takeyama J, Moriya T, Sasano H (2001) 5 alpha reductases in human breast carcinoma: possible modulator of in situ androgenic actions. J Clin Endocrinol Metab 86:2250–2257
29. Spinola PG, Marchetti B, Mérand Y, Bélanger A, Labrie F (1988) Effects of the aromatase inhibitor 4-hydroxyandrostenedione and the antiandrogen flutamide on growth and steroid levels in DMBA-induced rat mammary tumors. Breast Cancer Res Treat 12:287–296
30. Poulin R, Baker D, Labrie F (1988) Androgens inhibit basal and estrogen-induced cell proliferation in the ZR-75-1 human breast cancer cell line. Breast Cancer Res Treat 12:213–225
31. Van Gils CH, Onland-Moret C, Roest M, van Noord PAH, Peeters PHM (2003) The V89L polymorphism in the 5-α-reductase type 2 gene and risk of breast cancer. Cancer Epidemiol Biomark Prev 12:1194–1199
32. Van L-T, Bélanger A, Labrie F (2008) Androgen biosynthetic pathways in the human prostate. Best Pract Res Clin Endocrinol Metab 22(2):207–221
33. Wiebe JP, Lewis MJ, Cialacu V, Pawlak KJ, Zhang G (2005) The role of progesterone metabolites in breast cancer: potential for new diagnostics and therapeutics. J Steroid Biochem Mol Biol 93:201–208
34. Lewis MJ, Wiebe JP, Heathcote JG (2004) Expression of progesterone metabolizing genes (AKR1C1, AKR1C3, SRD5A1, SRD5A2) is altered in human breast carcinoma. BMC Cancer 4:27. doi:10.1186/1471-2407/4/27
35. Recchione C, Venturelli E, Manzari A, Cavalleri A, Martinetti A, Secreto G (1995) Testosterone, dihydrotestosterone and oestradiol levels in postmenopausal breast cancer tissues. J Steroid Biochem Mol Biol 52:541–546
36. Thiantanawat A, Long BJ, Brodie AM (2003) Signaling pathways of apoptosis activated by aromatase inhibitors and antiestrogens. Cancer Res 63:8037–8050

Cancer Science
The official journal of the Japanese Cancer Association JCA

Correlation between mammographic findings and corresponding histopathology: Potential predictors for biological characteristics of breast diseases

Kentaro Tamaki,[1,2,3,4] Takanori Ishida,[1] Minoru Miyashita,[1] Masakazu Amari,[1] Noriaki Ohuchi,[1] Nobumitsu Tamaki[3] and Hironobu Sasano[2]

[1]Department of Surgical Oncology, Tohoku University Graduate School of Medicine, Miyagi; [2]Department of Pathology, Tohoku University Hospital, Miyagi; [3]Department of Breast Surgery, Nahanishi Clinic, Okinawa, Japan

(Received July 21, 2011/Revised August 29, 2011/Accepted August 29, 2011/Accepted manuscript online September 2, 2011/Article first published online October 7, 2011)

The present study retrospectively evaluated the mammographic findings of 606 Japanese women with breast cancer (median age 50 years; range 27–89 years) and correlated them with histopathological characteristics. Mammographic findings were evaluated with an emphasis on mass shape, margin, density, calcification, and the presence of architectural distortion; these findings were correlated with histopathological characteristics such as intrinsic subtype, histological grade, lymphovascular invasion, and the Ki-67 labeling index. An irregular mass shape and masses with a spiculated margin were significantly higher in the group of patients with luminal A breast cancer than in patients with masses that were lobular or round, or in tumors with an indistinct or microlobulated periphery ($P = 0.017$, $P = 0.024$, $P < 0.001$, and $P = 0.001$, respectively). Irregular mass shape and spiculated periphery were significantly lower in patients with Grade 3 cancer ($P < 0.001$ for both). In terms of lymphovascular invasion, there were significant differences between oval and irregular or round mass shape ($P = 0.008$ and $P = 0.034$), between tumors with a microlobulated and indistinct periphery ($P = 0.014$), between tumors with a punctate and amorphous or pleomorphic calcification shape ($P = 0.030$ and 0.038), and between the presence and absence of architectural distortion ($P = 0.027$). Equivalent or low-density masses were also higher in Grade 1 breast cancers ($P = 0.007$). There were significant differences in the Ki-67 labeling index between irregular and lobular or round tumors ($P < 0.001$ and $P = 0.014$), as well as between spiculated and indistinct or microlobulated tumors ($P < 0.001$ for both). Significant differences were noted in the mammographic features of different primary breast cancer subtypes. These proposed mammographic diagnostic criteria based on biological characteristics may contribute to a more accurate prediction of biological behavior of breast malignancies. (*Cancer Sci* 2011; 102: 2179–2185)

The incidence of breast cancer has increased worldwide, which is considered due, in part, to mass screening programs resulting in the discovery of clinically occult breast lesions. Mammographic screening has been demonstrated to reduce breast cancer mortality in both Western and Oriental populations.[1] This mortality may be as great as 63% in women attending for screening.[2] Therefore, million of mammographic examinations are being performed yearly worldwide, and mammography has become the gold standard for detecting breast disorders. Strict attention to high-quality interpretation is required for successful of a mammographic diagnosis. Thus, it is important to establish an accurate diagnostic system for mammography.

Traditionally, prognostic determinations are made mainly on the basis of pathological information, including histological grade and lymphovascular invasion.[3–5] In addition to histological information, the status of molecular markers that have prognostic and predictive value can contribute to the selection of an optimal treatment strategy. These markers include estrogen receptor (ER), progesterone receptor (PgR), and human epidermal growth factor receptor 2 (HER2) and determining the status of these markers has become standard practice in the management of breast cancer because ER and HER2 positivity can predict a patient's response to endocrine therapy or targeted therapy with monoclonal antibodies directed against HER2.[6] In addition, the St Gallen international expert consensus meeting on the primary treatment of early breast cancer reported that features indicative of increased risk of recurrence, thus indirectly supporting the addition of chemotherapy to endocrine therapy, include lower expression of steroid hormone receptors, Grade 3 tumors, high proliferation (as measured by conventional or multigene assays), and extensive peritumoral vascular invasion.[7] However, these therapeutic determinations have been derived mainly from pathological information.

The appearance of tumors on mammograms has a generally good correlation with subsequent histological characteristics. For example, microcalcification is the hallmark of ductal carcinoma *in situ*;[8] spiculation is significantly correlated with low histologic grade; and ill-defined masses and microcalcifications are features of high-grade tumors.[8] Accurate correlation of mammographic findings with corresponding histopathologic features is considered one of the most important aspects of mammographic evaluation. Full histopathological information, including histological grades and intrinsic subtypes, is determined correctly after surgery.[9] Therefore, the purpose of the present study was to retrospectively evaluate mammographic findings and to compare the histopathological characteristics of the different tumors (i.e. intrinsic subtype, histological grade, lymphovascular invasion, and Ki-67 labeling index) in Japanese patients.

Materials and Methods

Patients. The mammographic and histopathologic features of 606 Japanese breast cancer patients who had undergone surgery at Tohoku University Hospital, Sendai, between January 2005 and June 2010 were reviewed retrospectively. All patients provided informed consent and the study protocol was approved by the Ethics Committee at Tohoku University Graduate School of Medicine. The median age of the patients was 50 years (range 27–89 years).

Imaging devices and breast tissue specimens. All mammographic examinations were performed with dedicated machines.

[4]To whom correspondence should be addressed.
E-mail: nahanisikenta@yahoo.co.jp

doi: 10.1111/j.1349-7006.2011.02088.x

Analog mammographic examinations were performed with one unit (MAMMOMAT 3000 Nova; Siemens, Erlangen, Germany) using a screen–film technique (Min-R 2000 Min-R EV; Kodak Health Imaging, Rochester, NY, USA). Digital mammograms were acquired by using a system with an amorphous selenium DirectRay digital detector (LOARD Selenia; Hologic, Waltham, MA, USA). The system was connected to a viewing monitor (MammoRead; TOYO, Tokyo, Japan).

Samples were stained using H&E. Histochemical and immunohistochemical analyses for ER, HER2, and Ki-67 were performed at the Department of Pathology, Tohoku University Hospital. Surgical specimens were fixed in 10% formaldehyde solution and cut into serial 5-mm slices, embedded in paraffin, cut into 4-μm sections, and placed on the glue-coated glass slides. We used the avidin–streptavidin immunoperoxidase method using the clone 6F11 antibody (Ventana, Tucson, AZ, USA) in an automated immunostainer (Benchmark System; Ventana). A standardized immunohistochemistry kit (Hercep-Test for Immunoenzymatic Staining; Dako, Copenhagen, Denmark) was used for HER2 staining. The Ki-67 labeling index was determined using an MIB-1 monoclonal antibody (code M7240; Dako). Both H&E and immunohistochemical staining were performed by a single experienced technician. Positive controls for ER and HER2 were breast carcinoma, whereas negative controls for immunostaining were hepatocellular carcinoma.

Imaging and histopathological analyses. Two experienced breast surgeons independently evaluated the mammographic findings. These two investigators were blinded as to the histopathological diagnosis and the clinical outcome of the patients. If there were discrepancies in the interpretation of the mammograms, a final decision was reached using consensus evaluations from eight experienced breast surgeons and radiologists. Mammographic findings were subsequently analyzed according to the American College of Radiology Breast Imaging Reporting and Data System (BI-RADS).[10] The presence of a mass, calcifications, focal asymmetric density (FAD), and architectural distortion were each recorded. Figure 1 shows representative mammographic findings. Mass shape was tentatively classified into round, oval, lobular, and irregular. Margins were classified as microlobulated, indistinct, spiculated, and "other". Density was classified into high, equivalent, or low. Calcification shape was tentatively classified into punctate, amorphous, pleomorphic, and linear. Finally, FAD was classified as with or without architectural distortion.

Two experienced pathologists independently evaluated surgical specimens. Histopathological evaluations were based on the World Health Organization (WHO) histological classification of tumors of breast and Rosen's Breast Pathology.[11,12] The presence of ER was determined by nuclear staining and was graded from 0 to 8 using the Allred score, with positivity defined as a score of ≥3.[13] With regard to HER2 evaluation, membranous staining was graded as 0–1+, 2+, and 3+.[14] Samples scored as 2+ were subjected to FISH to calculate the gene copy ratio of *HER2* to *CEP17* (PathVysion HER2 DNA Probe kit; Abbott, Chicago, IL, USA). Positivity was defined as a *HER2:CEP17*

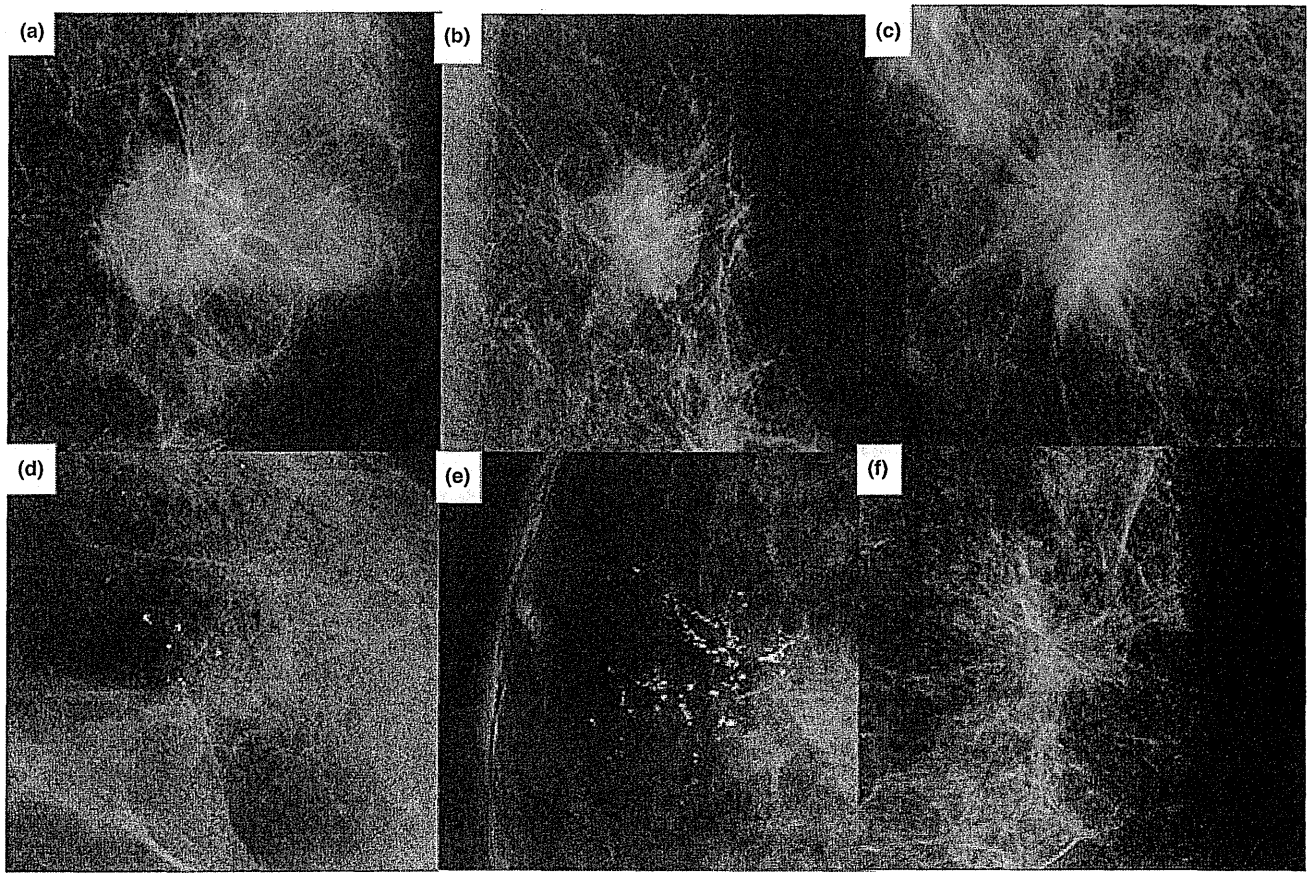

Fig. 1. Representative mammographic findings in breast carcinoma cases. (a) Round mass shape, microlobulated margin and intermediate density mass. (b) Lobular mass shape, indistinct margin, and high density mass. (c) Irregular mass shape, spiculated margin, and high-density mass. (d) Amorphous calcifications. (e) Pleomorphic or linear calcifications. (f) The presence of architectural distortion.

doi: 10.1111/j.1349-7006.2011.02088.x

signal ratio (FISH score) >2.2.[14] Histological grades were assessed according to the criteria of Elston and Ellis.[4] The Ki-67 immunoreactivity was evaluated by examining high-power fields and counting 1000 tumor cells in the hot spots.[15] In addition, the presence or absence of lymphovascular invasion was determined according to *Rosen's Breast Pathology*.[12] Intrinsic subtypes were classified according to the St Gallen international expert consensus on the primary therapy of early breast cancer 2011[16] as follows: luminal A was ER and/or PgR positive, HER2 negative, and Ki-67 low (<14%); luminal B was either ER and/or PgR positive, HER2 negative and Ki-67 high, or ER and/or PgR positive, any Ki-67, and HER2 over-expressed or amplified; the HER type was HER2 overexpressed or amplified and ER and PgR absent; and triple negative was ER, PgR and HER2 negative.

We compared mammographic findings, including mass shape, margin, density, calcification, FAD, and architectural distortion, with the histopathological characteristics of the tumors, including intrinsic subtype, histological grade, lymphovascular invasion, and the Ki-67 labeling index.

Statistical analysis. To compare mammographic findings with histopathological findings, multivariate analysis was used. All analyses were performed using SPSS version 10.0 (SPSS Inc., Chicago, IL, USA), with $P < 0.05$ taken to indicate significant differences.

Results

Comparison of mammographic findings with intrinsic subtype. Figure 2 summarizes the results of the numbers and ratios of each mammographic finding according to intrinsic subtype. In the luminal A group, significant differences were identified between masses that were irregular and lobular or round ($P = 0.017$ and $P = 0.024$), between those that had speculated and indistinct or microlobulated margins ($P < 0.001$ and $P = 0.001$), between those showing amorphous and pleomorphic calcification ($P = 0.044$), and between the presence and absence of architectural distortion ($P = 0.002$). In the HER group, significant differences were identified between masses that were irregular and oval or round ($P = 0.009$ and $P < 0.001$), between masses that were lobular and round ($P = 0.021$), and between those that had spiculated and microlobulated margins ($P = 0.005$). In the triple negative group, significant differences were identified between masses that had spiculated and

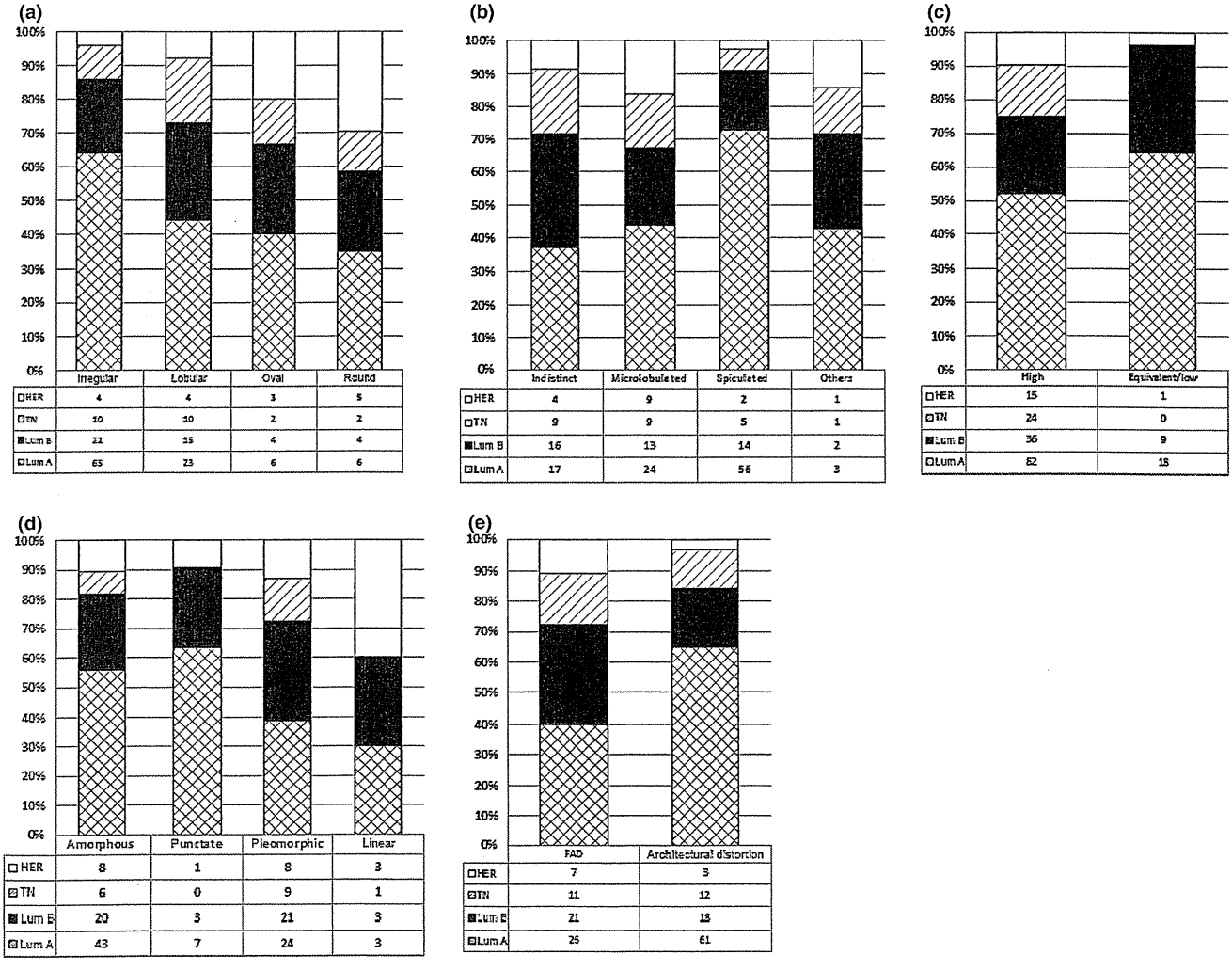

Fig. 2. Correlation between mammographic findings and intrinsic subtype: (a) mass shape, (b) margin, (c) density, (d) calcification shape, and (e) focal asymmetric density (FAD) and architectural distortion. HER, human epidermal growth factor receptor; TN, triple negative; Lum A, luminal A; Lum B, luminal B.

indistinct margins ($P = 0.027$), as well as between those identified as having high and equivalent or low density ($P = 0.027$).

Comparison of mammographic findings with histological grade. Figure 3 summarizes the results of the numbers and ratios of each mammographic finding according to histological grade. There were significant differences between irregular and lobular or oval mass shape in Grade 3 ($P < 0.001$ for all). Furthermore, in Grade 1 tumors, significant differences were found between with an indistinct and microlobulated or spiculated periphery ($P = 0.030$ and $P = 0.003$), between those with spiculated and indistinct or microlobulated margins ($P < 0.001$, respectively), between those identified as high and equivalent or low density ($P = 0.047$), and between those with a linear and amorphous calcification shape ($P = 0.027$).

Comparison of mammographic findings with lymphovascular invasion. Figure 4 summarizes the results for the numbers and ratios of each mammographic finding according to lymphovascular invasion. There were significant differences between oval and irregular or round mass shape ($P = 0.008$ and $P = 0.034$), between microlobulated and indistinct periphery ($P = 0.014$), between punctate and amorphous or pleomorphic calcification shape ($P = 0.030$ and 0.038), and between presence and absence of architectural distortion ($P = 0.027$).

Comparison of mammographic findings with the Ki-67 labeling index. Figure 5 summarizes the results of correlations between mammographic findings and the Ki-67 labeling index. The Ki-67 labeling index according to mass shape was 15.74 ± 6.21 for irregular masses, 38.82 ± 13.10 for lobular masses, 36.22 ± 15.75 for oval masses, and 37.85 ± 14.95 for round masses. According to mass periphery, the Ki-67 labeling index was 35.80 ± 28.51, 34.56 ± 29.76, 11.73 ± 10.86, and 27.50 ± 24.75 for tumors with indistinct, microlobulated, spiculated, and "other" margins, respectively. For tumors with a high and equivalent or low mass density, Ki-67 labeling index was 27.68 ± 26.75 and 13.14 ± 14.10, respectively. Tumors that showed amorphous, punctate, pleomorphic, and linear calcification had a Ki-67 labeling index of 24.55 ± 7.58, 26.00 ± 18.27, 24.68 ± 9.43, and 16.00 ± 17.23, respectively. In tumors without and with architectural distortion, the Ki-67 labeling index was 22.27 ± 8.64 and 25.02 ± 7.43, respectively. There were significant differences between irregular and lobular or round ($P < 0.001$ and $P = 0.014$), spiculated and indistinct or microlobulated ($P < 0.001$ for all), and high and equivalent or low density ($P = 0.018$) groups. A trend for a positive correlation was detected between irregular and oval mass shape, but the difference did not reach statistical significance ($P = 0.062$).

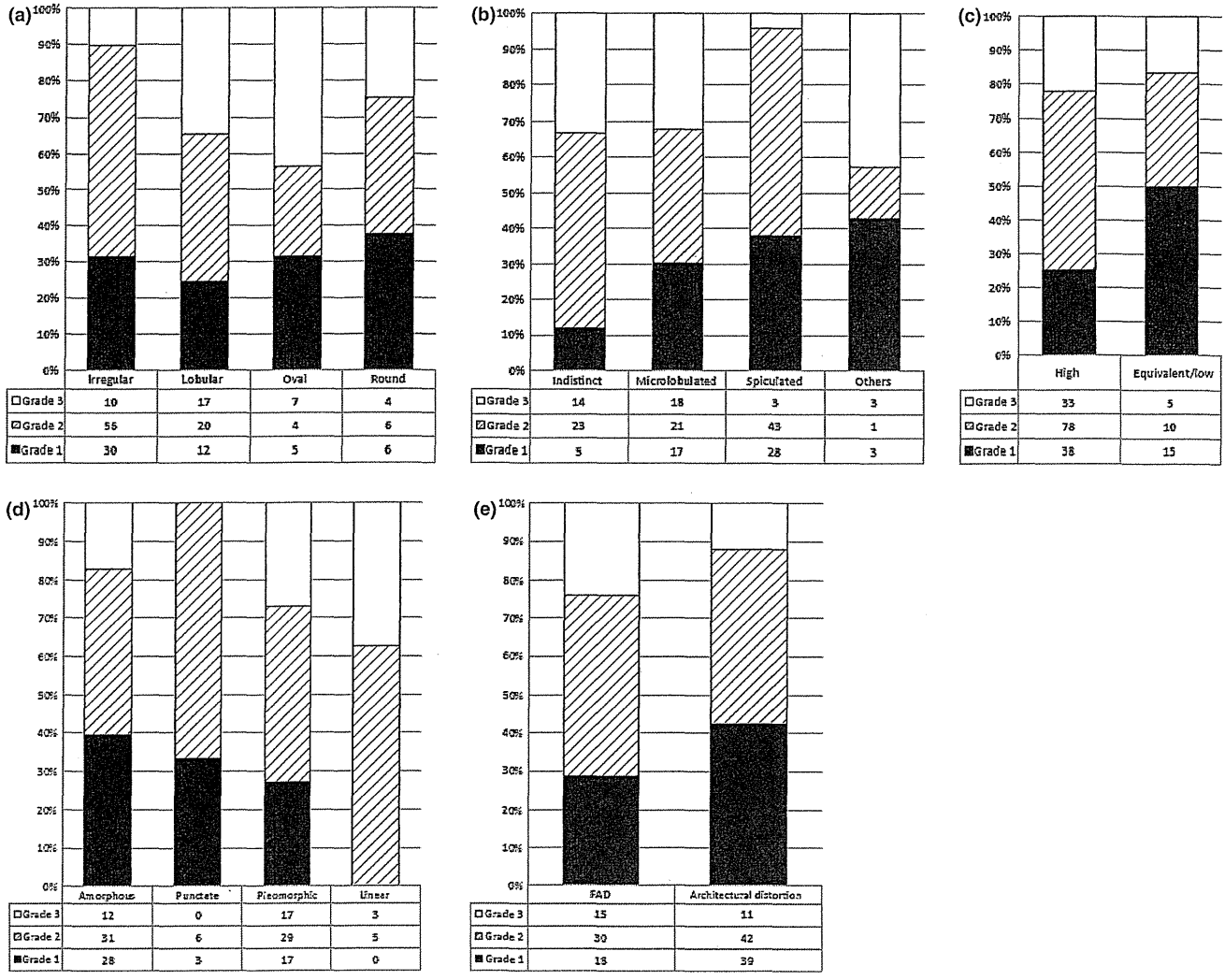

Fig. 3. Correlation between mammographic findings and histological grade: (a) mass shape, (b) margin, (c) density, (d) calcification shape, and (e) focal asymmetric density (FAD) and architectural distortion.

doi: 10.1111/j.1349-7006.2011.02088.x

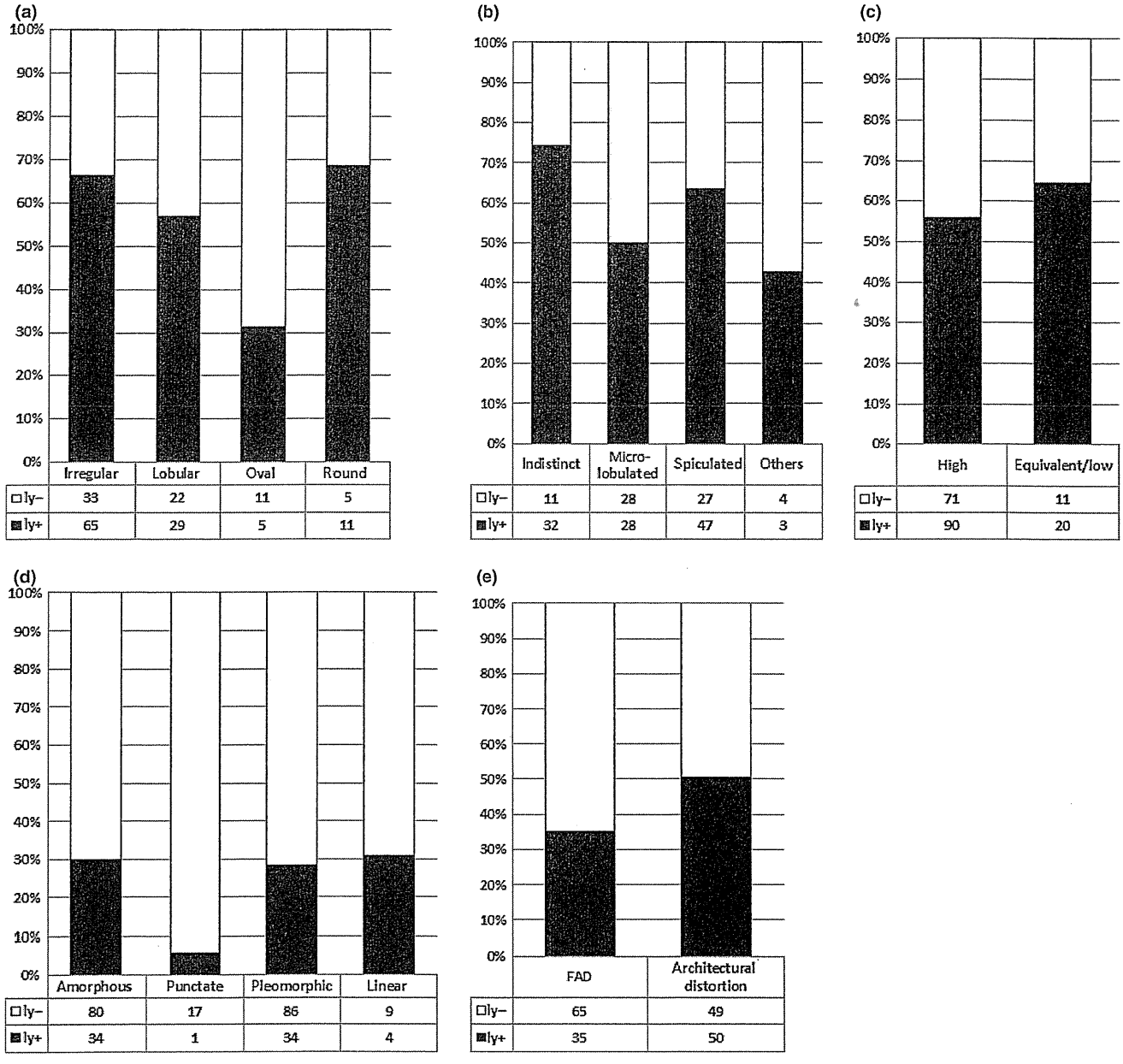

Fig. 4. Correlation between mammographic findings and lymphovascular invasion: (a) mass shape, (b) margin, (c) density, (d) calcification shape, and (e) focal asymmetric density (FAD) and architectural distortion. ly−, no lymphovascular invasion; ly+, lymphovascular invasion.

There were no significant differences according to calcification shape and the presence of architectural distortion.

Discussion

Histological grade is well known to have a strong correlation with clinical outcome in patients with breast cancer.[4] Accumulating clinical evidence suggests that prognostic factors influencing breast cancer extend beyond the traditional tumor histological grade.[17] Several factors, including ER expression, HER2 status, and lymphovascular invasion, have been clearly demonstrated in recent years to contribute significantly to the management and subsequent prognosis of patients with breast cancer.[7,18] Therefore, an accurate correlation between mammographic findings and their corresponding histopathological features is considered most important in mammographic evaluation. Mammographic findings may provide insights into pathological and biological features, including tumor cell characteristics, histological grade, and cell proliferation. We attempted to determine which finding is more relevant with regard to the newly defined subtype of breast carcinoma cells. Therefore, the purpose of the present study was to evaluate the correlation between mammographic findings (e.g. mass shape, margin, density, calcification shape, FAD, and the presence of architectural distortion) with intrinsic subtype, histological grade, lymphovascular invasion, and the Ki-67 labeling index in breast cancer patients.

Several previous studies evaluated the correlation between mammographic findings and histopathological characteristics in individual patients.[8,19–21] A number of independent groups demonstrated that masses with a spiculated periphery were associated with a good outcome in patients.[19,20] Conversely,

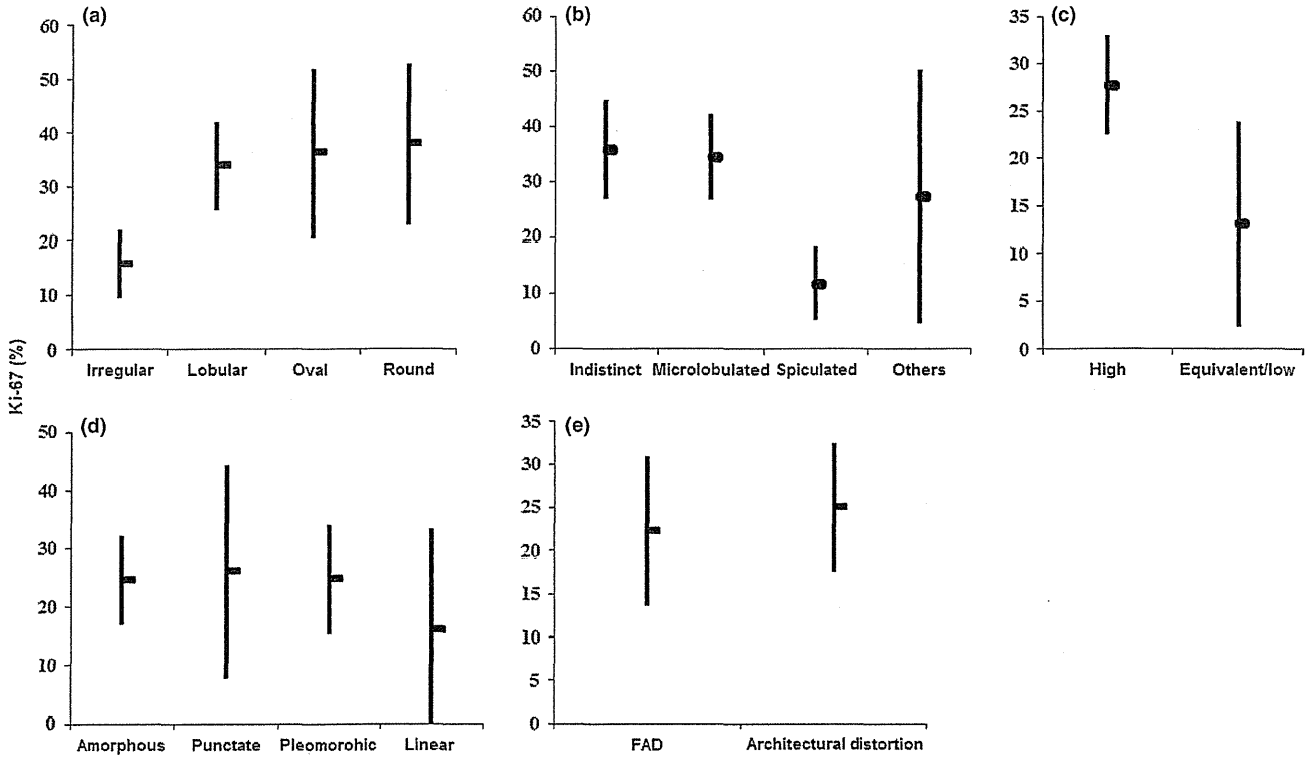

Fig. 5. Correlation between mammographic findings and Ki-67 labeling index: (a) mass shape, (b) margin, (c) density, (d) calcification shape, and (e) focal asymmetric density (FAD) and architectural distortion.

well-defined masses were associated with triple-negative breast cancer.[8,21] The results of the present study demonstrate that is a higher incidence of lower histological grade in masses with an irregular shape and/or spiculated margins, although a higher histological grade is not necessarily associated with irregular mass shape or spiculated margins. In addition, correlation of mammographic findings with the intrinsic subtype demonstrated that irregular mass shape and/or spiculated margin masses were significantly more frequently detected in luminal A breast cancers than in the other subtypes in this cohort of Japanese patients. However, oval and round mass shape and/or indistinct and microlobulated margin masses were significantly more frequently detected in triple-negative breast cancers or HER breast cancers. As for architectural distortion, the ratio of architectural distortion was significantly higher in luminal A cases and also tended to be associated with histological Grade 1. Together, these results suggest that poorly differentiated breast carcinoma cells are associated with good histological grade and luminal A subclassification. However, well-differentiated carcinoma cells are associated with adverse clinical grading and negative ER status.

Previous studies have demonstrated that these differentiations were related somewhat with adhesion factors.[22,23] Loss of adhesion factors in carcinoma cell is considered to play a role in the characteristic histological appearance of invasive carcinoma as loosely dispersed linear columns of cells and a typical discrete mass.[22] This more diffuse infiltrative pattern may explain some of the typical imaging appearances of tumors, such as spiculation and distortion.[22] In addition, adhesion factors are correlated with high histologic grade.[23] Therefore, adhesion factors may be considered to be correlated with the results of the present study in that spiculated breast cancers have a good clinical outcome and histological Grade 1. However, it is also true that numerous biological mechanisms underlying the association between the process of infiltration and histopathological characteristics remain unknown and that further investigations are required to confirm interpretation of mammography in terms of the biological and histopathologic characteristics of tumors.

To the best of our knowledge, this is the first study to compare mammographic findings with the Ki-67 labeling index and histopathological lymphovascular invasion. The results of the present study demonstrated that there was a higher incidence of a lower Ki-67 labeling index in tumors with an irregular mass shape, spiculated periphery, and equivalent or low mass density. Irregular mass shape and a spiculated periphery are well-known predictors of malignancy, but the results of the present study seem to suggest that findings of irregular shape and a spiculated periphery are relatively good prognostic predictors in terms of the Ki-67 labeling index. In addition, the results of the present study demonstrate that lymphovascular invasion was significantly greater in cases in which there was architectural distortion; however, the incidence of lymphovascular invasion was not significantly higher in spiculated masses. These results all suggest that the correlation between findings of radiological dist ortion and the mechanisms of lymphovascular invasion remain unknown and further investigations are required.

We also examined the correlation between mammographic calcification shape and histopathological characteristics. Previous studies have reported that triple-negative breast cancers are more likely to exhibit comedo calcifications.[8] In addition, the high frequency of comedo calcification in triple-negative breast cancers may represent a consequence of high histologic grade.[8] The presence of mammographic comedo calcification has also been reported to be associated with a poor prognosis in small screening-detected invasive cancers.[19] The results of the present study also demonstrate that non-necrotic calcifications, including amorphous and punctate calcification, are associated with a higher ratio of luminal A cases, whereas necrotic calcifications, including pleomorphic and linear calcification, were

doi: 10.1111/j.1349-7006.2011.02088.x

associated with a higher ratio of HER breast cancers. In addition, necrotic calcifications tended to be associated with a higher histological grade than non-necrotic calcifications. Therefore, the results suggest that the type of calcification may become a prognostic factor for breast malignancies.

We noted significant differences in the mammographic features of different primary breast cancer immunophenotypes in the present study. Stratifying the mammographic features according to immunophenotypes reveals distinct differences among cancer subtypes. However, the limitations of the present study include that fact that the study was retrospective in nature and was performed in a single institute, namely Tohoku University Hospital. Therefore, further investigations are needed, including analysis in several different institutions to further refine the new mammographic criteria. Biological and histopathological differences may result in imaging differences that may help us better understand the development of breast cancer. These proposed mammographic diagnostic criteria based on biological characteristics may contribute to a more accurate prediction of the biological behavior of breast malignancies.

Acknowledgments

The authors thank medical technologist Mr Masahiro Sai for his excellent technical assistance for mammography. The authors also thank medical technologist Ms Yayoi Takahashi for excellent technical assistance with the immunohistochemical staining. This work was supported, in part, by a Grant-in Aid from Kurokawa Cancer Research Foundation.

Disclosure Statement

The authors have no conflict of interest.

References

1 Nystrom L, Rutqvist L, Wall S *et al.* Breast cancer screening with mammography; overview of Swedish randomized trials. *Lancet* 1993; **341**: 973–8.
2 Tabar L, Vitak B, Chen HH *et al.* Beyond randomized controlled trials: organized mammographic screening substantially reduces breast carcinoma mortality. *Cancer* 2001; **91**: 1724–31.
3 Carter CL, Allen C, Henson DE. Relation of tumour size, lymph node status, and survival in 24,740 breast cancer cases. *Cancer* 1989; **63**: 181–7.
4 Elston CW, Ellis IO. Pathological prognostic factors in breast cancer. I. The value of histological grade in breast cancer: experience from a large study with long-term follow-up. *Histopathology* 1991; **19**: 403–10.
5 Lee AHS, Pinder SE, Macmillan RD *et al.* Prognostic value of lymph vascular invasion in women with lymph node negative invasive breast carcinoma. *Eur J Cancer* 2006; **42**: 357–62.
6 Bauer KR, Brown M, Cress RD *et al.* Descriptive analysis of estrogen receptor (ER)-negative, progesterone receptor (PR)-negative, and HER2-negative invasive breast cancer, the so-called triple-negative phenotype: a population-based study from the California Cancer Registry. *Cancer* 2007; **109**: 1721–8.
7 Goldhirsch A, Ingle JN, Gelber RD *et al.* Thresholds for therapies: highlights of the St Gallen international expert consensus on the primary therapy of early breast cancer 2009. *Ann Oncol* 2009; **20**: 1319–29.
8 Luck AA, Evans AJ, James JJ *et al.* Breast carcinoma with basal phenotype: mammographic findings. *AJR Am J Roentgenol* 2008; **191**: 346–51.
9 Tamaki K, Sasano H, Ishida T *et al.* Comparison of core needle biopsy (CNB) and surgical specimens for accurate preoperative evaluation of ER, PgR and HER2 status of breast cancer patients. *Cancer Sci* 2010; **101**: 2074–9.
10 D'Orsi CJ, Bassett LW, Berg WA *et al. Breast Imaging Reporting and Data System: ACR BI-RADS-Mammography*, 4th edn. Reston, Virginia: American College of Radiology, 2003.
11 Tavassoli FA, Devilee P. *World Health Organization Classification of Tumors. Tumor of the Breast and Females Gentia Organs.* Lyon: IARC Press, 2003.
12 Rosen PP. *Rosen's Breast Pathology*, 3rd edn. Philadelphia: Lippincott Williams & Wilkins, 2009.
13 Allred DC, Harvey JM, Berardo M, Clark GM. Prognostic and predictive factors in breast cancer by immunohistochemical analysis. *Mod Pathol* 1998; **11**: 155–68.
14 Wolff AC, Hammond MH, Schwartz JN *et al.* American Society of Clinical Oncology/College of American Pathologists guideline recommendations for human epidermal growth factor receptor 2 testing in breast cancer. *J Clin Oncol* 2007; **25**: 118–45.
15 Spyratos F, Ferrero-Pous M, Trassard M *et al.* Correlation between MIB-1 and other proliferation marker clinical implications of the MIB-1 cutoff value. *Cancer* 2002; **94**: 2151–9.
16 Goldhirsch A, Wood WC, Coates AS *et al.* Strategies for subtypes-dealing with the diversity of breast cancer: highlights of the St Gallen International Expert Consensus on the Primary Therapy of Early Breast Cancer 2011. *Ann Oncol* 2011; **22**: 1736–47.
17 Taneja S, Evans AJ, Rakha EA *et al.* The mammographic correlations of a new immunohistochemical classification of invasive breast cancer. *Clin Radiol* 2008; **63**: 1228–35.
18 Jalava P, Kuopio T, Juntti-Patinen L *et al.* Ki67 immunohistochemistry: a valuable marker in prognostication but with a risk of misclassification: proliferation subgroups formed based on Ki67 immunoreactivity and standardized mitotic index. *Histopathology* 2006; **48**: 674–82.
19 Tabar L, Tony Chen HH, Amy Yen MF *et al.* Mammographic tumor features can predict long-term outcomes reliably in women with 1–14-mm invasive breast carcinoma. *Cancer* 2004; **101**: 1745–59.
20 Evan AJ, Pinder SE, James JJ *et al.* Is mammographic spiculation an independent, good prognostic factor in screening detected invasive breast cancer? *AJR Am J Roentgenol* 2006; **187**: 1377–80.
21 Ko ES, Lee BH, Kim HA *et al.* Triple-negative breast cancer: correlation between imaging and pathological findings. *Eur Radiol* 2010; **20**: 1111–7.
22 Doyle S, Evans AJ, Rakha EA *et al.* Influence of E-cadherin expression on the mammographic appearance of invasive nonlobular breat carcinoma detected at screening. *Radiology* 2009; **253**: 51–5.
23 Gastl G, Spizzo G, Obrist P *et al.* Ep-CAM overexpression in breast cancer as a predictor of survival. *Lancet* 2000; **356**: 1981–2.

Cancer Science
The official journal of the Japanese Cancer Association

Correlation between mammographic findings and corresponding histopathology: Potential predictors for biological characteristics of breast diseases

Kentaro Tamaki,[1,2,3,4] Takanori Ishida,[1] Minoru Miyashita,[1] Masakazu Amari,[1] Noriaki Ohuchi,[1] Nobumitsu Tamaki[3] and Hironobu Sasano[2]

[1]Department of Surgical Oncology, Tohoku University Graduate School of Medicine, Miyagi; [2]Department of Pathology, Tohoku University Hospital, Miyagi; [3]Department of Breast Surgery, Nahanishi Clinic, Okinawa, Japan

(Received July 21, 2011/Revised August 29, 2011/Accepted August 29, 2011/Accepted manuscript online September 2, 2011/Article first published online October 7, 2011)

The present study retrospectively evaluated the mammographic findings of 606 Japanese women with breast cancer (median age 50 years; range 27–89 years) and correlated them with histopathological characteristics. Mammographic findings were evaluated with an emphasis on mass shape, margin, density, calcification, and the presence of architectural distortion; these findings were correlated with histopathological characteristics such as intrinsic subtype, histological grade, lymphovascular invasion, and the Ki-67 labeling index. An irregular mass shape and masses with a spiculated margin were significantly higher in the group of patients with luminal A breast cancer than in patients with masses that were lobular or round, or in tumors with an indistinct or microlobulated periphery ($P = 0.017$, $P = 0.024$, $P < 0.001$, and $P = 0.001$, respectively). Irregular mass shape and spiculated periphery were significantly lower in patients with Grade 3 cancer ($P < 0.001$ for both). In terms of lymphovascular invasion, there were significant differences between oval and irregular or round mass shape ($P = 0.008$ and $P = 0.034$), between tumors with a microlobulated and indistinct periphery ($P = 0.014$), between tumors with a punctate and amorphous or pleomorphic calcification shape ($P = 0.030$ and 0.038), and between the presence and absence of architectural distortion ($P = 0.027$). Equivalent or low-density masses were also higher in Grade 1 breast cancers ($P = 0.007$). There were significant differences in the Ki-67 labeling index between irregular and lobular or round tumors ($P < 0.001$ and $P = 0.014$), as well as between spiculated and indistinct or microlobulated tumors ($P < 0.001$ for both). Significant differences were noted in the mammographic features of different primary breast cancer subtypes. These proposed mammographic diagnostic criteria based on biological characteristics may contribute to a more accurate prediction of biological behavior of breast malignancies. (*Cancer Sci* 2011; 102: 2179–2185)

The incidence of breast cancer has increased worldwide, which is considered due, in part, to mass screening programs resulting in the discovery of clinically occult breast lesions. Mammographic screening has been demonstrated to reduce breast cancer mortality in both Western and Oriental populations.[1] This mortality may be as great as 63% in women attending for screening.[2] Therefore, million of mammographic examinations are being performed yearly worldwide, and mammography has become the gold standard for detecting breast disorders. Strict attention to high-quality interpretation is required for successful of a mammographic diagnosis. Thus, it is important to establish an accurate diagnostic system for mammography.

Traditionally, prognostic determinations are made mainly on the basis of pathological information, including histological grade and lymphovascular invasion.[3–5] In addition to histological information, the status of molecular markers that have prognostic and predictive value can contribute to the selection of an optimal treatment strategy. These markers include estrogen receptor (ER), progesterone receptor (PgR), and human epidermal growth factor receptor 2 (HER2) and determining the status of these markers has become standard practice in the management of breast cancer because ER and HER2 positivity can predict a patient's response to endocrine therapy or targeted therapy with monoclonal antibodies directed against HER2.[6] In addition, the St Gallen international expert consensus meeting on the primary treatment of early breast cancer reported that features indicative of increased risk of recurrence, thus indirectly supporting the addition of chemotherapy to endocrine therapy, include lower expression of steroid hormone receptors, Grade 3 tumors, high proliferation (as measured by conventional or multigene assays), and extensive peritumoral vascular invasion.[7] However, these therapeutic determinations have been derived mainly from pathological information.

The appearance of tumors on mammograms has a generally good correlation with subsequent histological characteristics. For example, microcalcification is the hallmark of ductal carcinoma *in situ*;[8] spiculation is significantly correlated with low histologic grade; and ill-defined masses and microcalcifications are features of high-grade tumors.[8] Accurate correlation of mammographic findings with corresponding histopathologic features is considered one of the most important aspects of mammographic evaluation. Full histopathological information, including histological grades and intrinsic subtypes, is determined correctly after surgery.[9] Therefore, the purpose of the present study was to retrospectively evaluate mammographic findings and to compare the histopathological characteristics of the different tumors (i.e. intrinsic subtype, histological grade, lymphovascular invasion, and Ki-67 labeling index) in Japanese patients.

Materials and Methods

Patients. The mammographic and histopathologic features of 606 Japanese breast cancer patients who had undergone surgery at Tohoku University Hospital, Sendai, between January 2005 and June 2010 were reviewed retrospectively. All patients provided informed consent and the study protocol was approved by the Ethics Committee at Tohoku University Graduate School of Medicine. The median age of the patients was 50 years (range 27–89 years).

Imaging devices and breast tissue specimens. All mammographic examinations were performed with dedicated machines.

[4]To whom correspondence should be addressed.
E-mail: nahanisikenta@yahoo.co.jp

doi: 10.1111/j.1349-7006.2011.02088.x

Analog mammographic examinations were performed with one unit (MAMMOMAT 3000 Nova; Siemens, Erlangen, Germany) using a screen–film technique (Min-R 2000 Min-R EV; Kodak Health Imaging, Rochester, NY, USA). Digital mammograms were acquired by using a system with an amorphous selenium DirectRay digital detector (LOARD Selenia; Hologic, Waltham, MA, USA). The system was connected to a viewing monitor (MammoRead; TOYO, Tokyo, Japan).

Samples were stained using H&E. Histochemical and immunohistochemical analyses for ER, HER2, and Ki-67 were performed at the Department of Pathology, Tohoku University Hospital. Surgical specimens were fixed in 10% formaldehyde solution and cut into serial 5-mm slices, embedded in paraffin, cut into 4-μm sections, and placed on the glue-coated glass slides. We used the avidin–streptavidin immunoperoxidase method using the clone 6F11 antibody (Ventana, Tucson, AZ, USA) in an automated immunostainer (Benchmark System; Ventana). A standardized immunohistochemistry kit (Hercep-Test for Immunoenzymatic Staining; Dako, Copenhagen, Denmark) was used for HER2 staining. The Ki-67 labeling index was determined using an MIB-1 monoclonal antibody (code M7240; Dako). Both H&E and immunohistochemical staining were performed by a single experienced technician. Positive controls for ER and HER2 were breast carcinoma, whereas negative controls for immunostaining were hepatocellular carcinoma.

Imaging and histopathological analyses. Two experienced breast surgeons independently evaluated the mammographic findings. These two investigators were blinded as to the histopathological diagnosis and the clinical outcome of the patients. If there were discrepancies in the interpretation of the mammograms, a final decision was reached using consensus evaluations from eight experienced breast surgeons and radiologists. Mammographic findings were subsequently analyzed according to the American College of Radiology Breast Imaging Reporting and Data System (BI-RADS).[10] The presence of a mass, calcifications, focal asymmetric density (FAD), and architectural distortion were each recorded. Figure 1 shows representative mammographic findings. Mass shape was tentatively classified into round, oval, lobular, and irregular. Margins were classified as microlobulated, indistinct, spiculated, and "other". Density was classified into high, equivalent, or low. Calcification shape was tentatively classified into punctate, amorphous, pleomorphic, and linear. Finally, FAD was classified as with or without architectural distortion.

Two experienced pathologists independently evaluated surgical specimens. Histopathological evaluations were based on the World Health Organization (WHO) histological classification of tumors of breast and Rosen's Breast Pathology.[11,12] The presence of ER was determined by nuclear staining and was graded from 0 to 8 using the Allred score, with positivity defined as a score of ≥3.[13] With regard to HER2 evaluation, membranous staining was graded as 0–1+, 2+, and 3+.[14] Samples scored as 2+ were subjected to FISH to calculate the gene copy ratio of *HER2* to *CEP17* (PathVysion HER2 DNA Probe kit; Abbott, Chicago, IL, USA). Positivity was defined as a *HER2*:*CEP17*

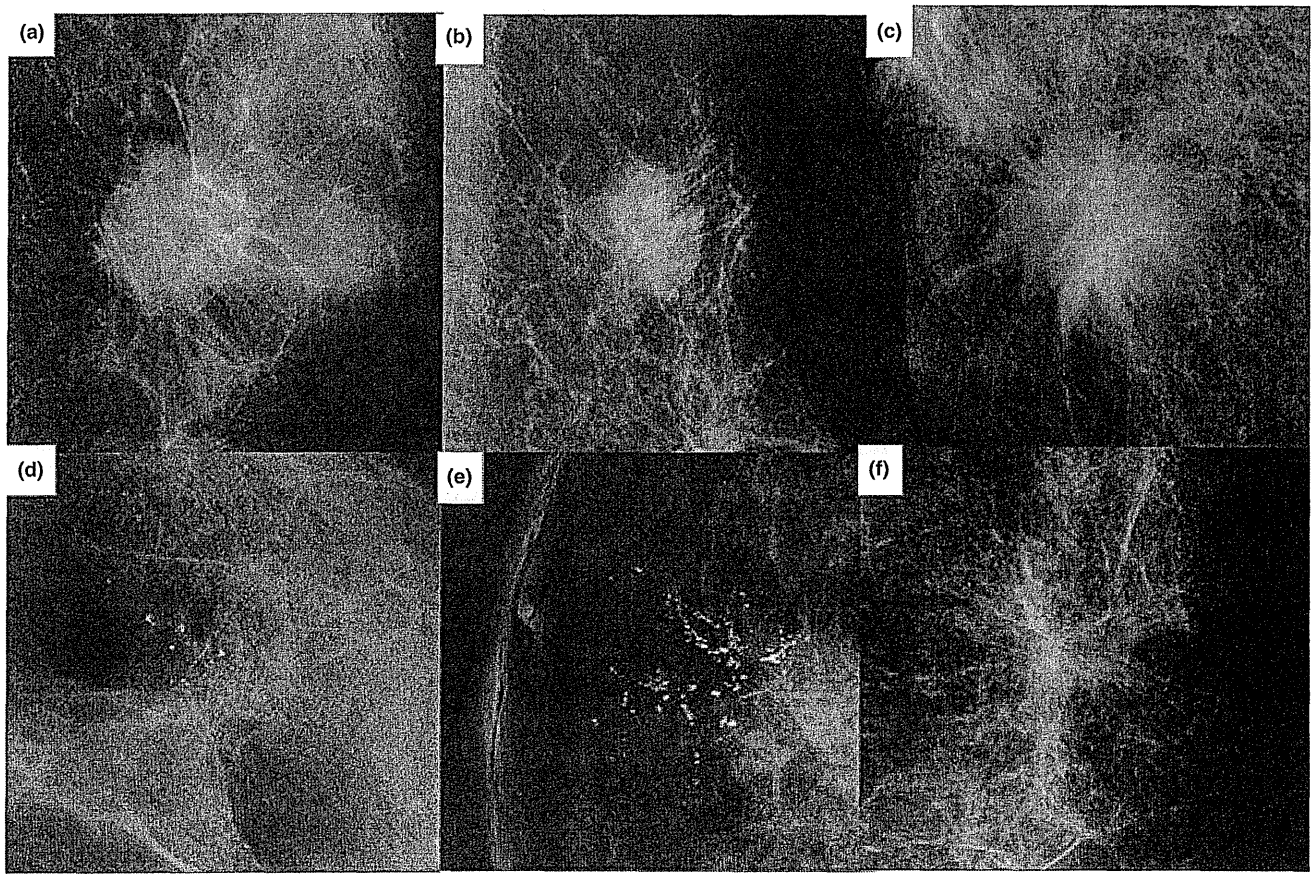

Fig. 1. Representative mammographic findings in breast carcinoma cases. (a) Round mass shape, microlobulated margin and intermediate density mass. (b) Lobular mass shape, indistinct margin, and high density mass. (c) Irregular mass shape, spiculated margin, and high-density mass. (d) Amorphous calcifications. (e) Pleomorphic or linear calcifications. (f) The presence of architectural distortion.

doi: 10.1111/j.1349-7006.2011.02088.x

signal ratio (FISH score) >2.2.[14] Histological grades were assessed according to the criteria of Elston and Ellis.[4] The Ki-67 immunoreactivity was evaluated by examining high-power fields and counting 1000 tumor cells in the hot spots.[15] In addition, the presence or absence of lymphovascular invasion was determined according to *Rosen's Breast Pathology*.[12] Intrinsic subtypes were classified according to the St Gallen international expert consensus on the primary therapy of early breast cancer 2011[16] as follows: luminal A was ER and/or PgR positive, HER2 negative, and Ki-67 low (<14%); luminal B was either ER and/or PgR positive, HER2 negative and Ki-67 high, or ER and/or PgR positive, any Ki-67, and HER2 overexpressed or amplified; the HER type was HER2 overexpressed or amplified and ER and PgR absent; and triple negative was ER, PgR and HER2 negative.

We compared mammographic findings, including mass shape, margin, density, calcification, FAD, and architectural distortion, with the histopathological characteristics of the tumors, including intrinsic subtype, histological grade, lymphovascular invasion, and the Ki-67 labeling index.

Statistical analysis. To compare mammographic findings with histopathological findings, multivariate analysis was used. All analyses were performed using SPSS version 10.0 (SPSS Inc., Chicago, IL, USA), with $P < 0.05$ taken to indicate significant differences.

Results

Comparison of mammographic findings with intrinsic subtype. Figure 2 summarizes the results of the numbers and ratios of each mammographic finding according to intrinsic subtype. In the luminal A group, significant differences were identified between masses that were irregular and lobular or round ($P = 0.017$ and $P = 0.024$), between those that had speculated and indistinct or microlobulated margins ($P < 0.001$ and $P = 0.001$), between those showing amorphous and pleomorphic calcification ($P = 0.044$), and between the presence and absence of architectural distortion ($P = 0.002$). In the HER group, significant differences were identified between masses that were irregular and oval or round ($P = 0.009$ and $P < 0.001$), between masses that were lobular and round ($P = 0.021$), and between those that had spiculated and microlobulated margins ($P = 0.005$). In the triple negative group, significant differences were identified between masses that had spiculated and

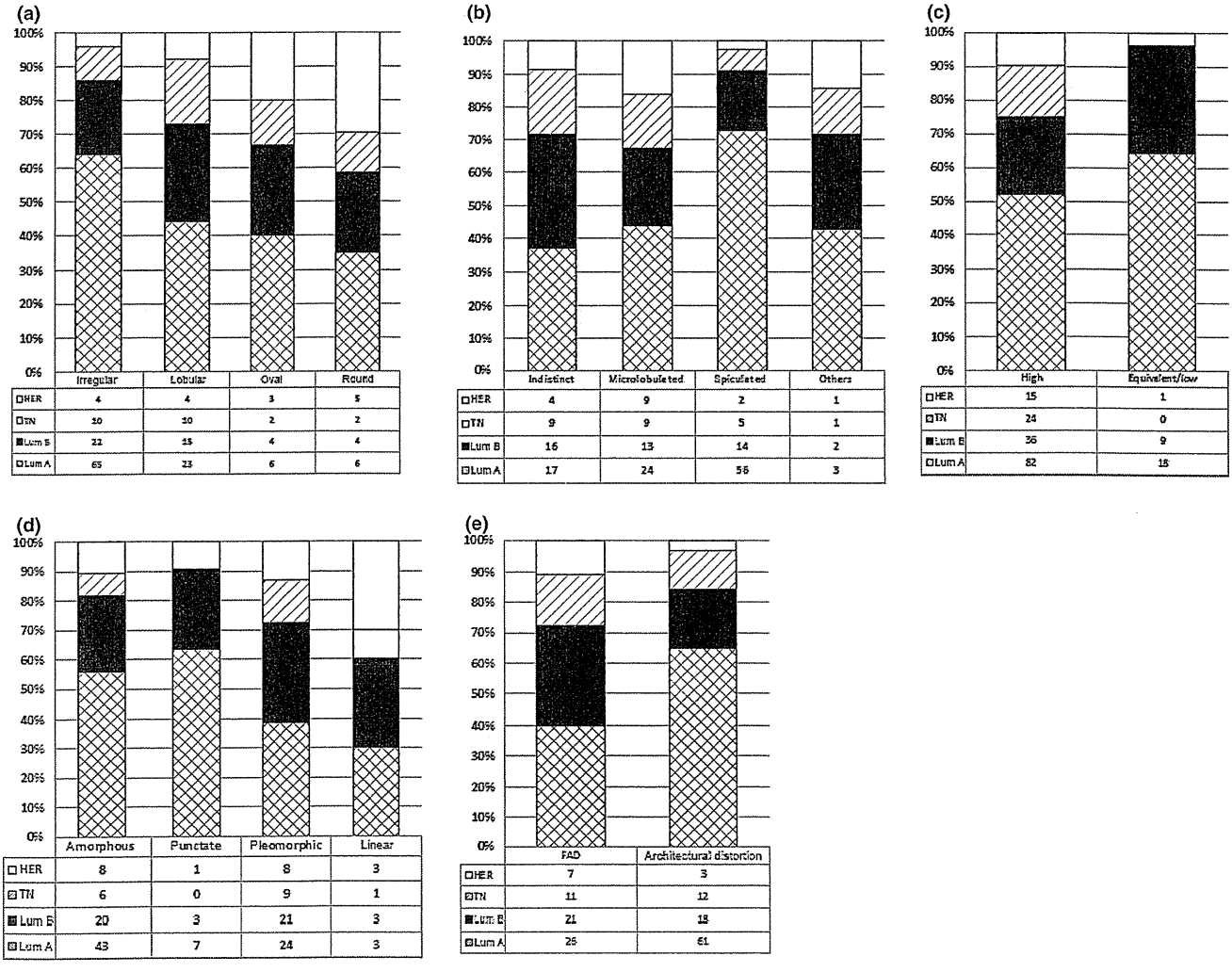

Fig. 2. Correlation between mammographic findings and intrinsic subtype: (a) mass shape, (b) margin, (c) density, (d) calcification shape, and (e) focal asymmetric density (FAD) and architectural distortion. HER, human epidermal growth factor receptor; TN, triple negative; Lum A, luminal A; Lum B, luminal B.